

GABRIELA LOPES FERNANDES

**Nanopartículas de prata e glicerofosfato de cálcio:
sínteses por rotas convencionais e fitoquímica, análise
antimicrobiana e avaliação da citotoxicidade**

Araçatuba
2016

GABRIELA LOPES FERNANDES

**Nanopartículas de prata e glicerofosfato de cálcio:
sínteses por rotas convencionais e fitoquímica, análise
antimicrobiana e avaliação da citotoxicidade**

Dissertação apresentada à Faculdade de Odontologia do Campus de Araçatuba – Universidade Estadual Paulista “Júlio de Mesquita Filho”- UNESP, para obtenção do Título de MESTRE EM CIÊNCIA ODONTOLÓGICA (Área de concentração em Biomateriais).

Orientadora: Prof^ª. Ass. Dr^ª. Debora de Barros Barbosa

Co-Orientador: Pós-doc Aline Satie Takamiya

Araçatuba - SP

2016

Catálogo na Publicação (CIP)
Diretoria Técnica de Biblioteca e Documentação – FOA / UNESP

Fernandes, Gabriela Lopes.
F363e Nanopartículas de prata e glicerofosfato de cálcio: sínteses
por rotas convencionais e fitoquímica, análise antimicrobiana
e avaliação da citotoxicidade / Gabriela Lopes Fernandes. -
Araçatuba, 2016
104 f. : 13 il. ; 4 tab. + 1 CD-ROM

Dissertação (Mestrado) – Universidade Estadual Paulista,
Faculdade de Odontologia de Araçatuba
Orientadora: Profa. Débora Barros Barbosa
Coorientadora: Dra. Aline Satie Takamiya

1. Nanopartículas 2. Punicaceae 3. Candida albicans
4. Streptococcus mutans 5. Citotoxicidade celular I. T.

Black D15
CDD 617.6

DADOS CURRICULARES

GABRIELA LOPES FERNANDES

NASCIMENTO	01/11/1990 – GENERAL SALGADO – SP
FILIAÇÃO	Carlos Braz Fernandes Maria Lúcia Lopes Fernandes
2009/2013	Curso de Graduação em Odontologia Faculdade de Odontologia de Araçatuba - Universidade Estadual Paulista “Júlio de Mesquita Filho”.
2013/2013	Curso de Aperfeiçoamento em Prótese Parcial Fixa Faculdade de Odontologia de Araçatuba - Universidade Estadual Paulista “Júlio de Mesquita Filho”.
2013/2013	Aperfeiçoamento em Endodontia automatizada. Faculdade de Odontologia de Araçatuba - Universidade Estadual Paulista “Júlio de Mesquita Filho”.

DEDICATÓRIA

Aos meus amados pais, Maria Lucia Lopes Fernandes e Carlos Braz Fernandes

Dedico este título a vocês, não poderia dedicar a mais ninguém senão a vocês. Agradeço por todas as vezes que deixaram de viver seus sonhos para dar a mim todos os recursos possíveis e imagináveis para que eu realizasse todos os meus sonhos. Vocês são o maior tesouro que possuo, o que já fizeram por mim jamais poderei pagar com bens materiais. Vocês são minha base, meu passado, presente e futuro, pai e mãe, obrigada por existir, amo vocês!

Aos meus avós, Assunta de Rico Lopes , Sebastião Lopes, Isolina Fernandes e Joaquim Fernandes (in memorian)

A quem eu tenho imenso carinho, admiração e respeito. Em especial, a minha “vó Sunta”, obrigada por ainda cuidar tanto de mim como na minha infância, com toda certeza a sua casa e o seu abraço vão sempre ser um dos meus lugares favoritos.

Aos meus tios Maria Rosa Lopes e Osvaldo Marques Junior e primos João Pedro Marques e Gabriel Henrique Marques

Minha segunda família onde tenho a certeza de sempre poder contar, a vocês meus tios, eu devo todo o respeito e carinho de pais, e aos meus primos todo o amor e confiança de irmãos.

AGRADECIMENTOS ESPECIAIS

A Deus

Agradeço a Deus por todas as maravilhas que ele realiza em minha vida a todo momento, mas agradeço ao Senhor principalmente por ele permitir que eu o conheça cada vez mais, não há realização maior em poder sentir o poder de Deus, em saber que a sua misericórdia por todos nós é eterna. Obrigada Pai, em ti eu sei que nunca estou só.

À minha orientadora, Prof^a. Ass. Dr^a. Débora Barros Barbosa

Eu sou imensamente grata a Deus por sua vida professora, a senhora com certeza é uma das melhores pessoas que eu já conheci, justa, honesta, sempre nos incentivando a ser melhores e a tirar as melhores conclusões de todas as situações. Obrigada não só por ser a melhor orientadora que eu poderia ter na Pós-graduação, mas por me orientar na vida, com certeza eu sigo o seu exemplo profissional, mas também o exemplo de como podemos ser um ser humano melhor.

Ao Prof. Dr. Emerson Rodrigues, Dr. Luiz Fernando Gorup e Dr. Franciso Nunes

Neto

Sem a imensa colaboração de vocês com certeza esse trabalho não seria possível, sou extremamente grata por todas as vezes que ficaram a minha disposição para aprimorar os resultados deste trabalho, é um prazer e uma satisfação enorme participar desta equipe de pesquisa tão sólida e eficiente.

À Prof^ª Dr.^a Margarete Tereza Gottardo Almeida e ao Dr. Douglas Roberto Monteiro

Por aceitarem o convite para fazer parte da Banca Examinadora, e principalmente por serem pessoas que eu admiro muito profissionalmente.

À Fundação de Ampara à Pesquisa do Estado de São Paulo (FAPESP)

Pelo grande incentivo na forma de Bolsa de Mestrado (FAPESP, Processo 2014/08648 2) e Auxílio Financeiro (FAPESP, Processo 2013/24200-9)

Ao Conselho Nacional de Desenvolvimento Científico e Tecnológico (CAPES)

Pelo grande incentivo na forma de Auxílio Financeiro (Processo 88887.068358/2014-00 e 88881.030445/2013-01).

AGRADECIMENTOS

À *Faculdade de Odontologia de Araçatuba - UNESP*, na pessoa de seu diretor *Prof. Tit. Wilson Roberto Poi*, pela oportunidade de aprendizado e crescimento pessoal e profissional.

À *Universidade Federal de São Carlos - UFSCar*, nas dependências do Laboratório Interdisciplinar de Eletroquímica e Cerâmica do Departamento de Química, onde foi possível realizar todas às sínteses propostas no trabalho.

À *APIS FLORA INDUSTRIAL E COMERCIAL LTDA*, onde parte fundamental deste trabalho foi realizado com a ajuda de extrema importância de alguns dos alunos e funcionários.

À *Faculdade de Ciências Farmacêuticas de Ribeirão Preto - USP*, na pessoa da *Prof^{ra} Dr^a. Maria José Vieira Fonseca*, por abrir as portas do seu laboratório para o desenvolvimento de parte do trabalho, muito obrigada.

Ao atual *coordenador do Programa de Pós-graduação em Ciência odontologica*, da Faculdade de Odontologia de Araçatuba - UNESP, *Prof. Adj. Luciano Tavares Angelo Cintra*, pela competência e acessibilidade.

Ao *Departamento de Materiais Odontológicos e Prótese* da Faculdade de Odontologia de Araçatuba - UNESP, representado por todos os seus *Funcionários*, pelo convívio agradável.

Ao *Departamento de Odontopediatria* da Faculdade de Odontologia de Araçatuba - UNESP, representado por todos os seus *Professores* e *Funcionários*, pela oportunidade de realizar meu mestrado e conviver com pessoas tão agradáveis.

Ao *Prof. Titular Alberto Carlos Botazzo Delbem*, por toda contribuição não só material, mas também intelectual que me proporcionou nesses últimos anos, com toda certeza aprendi muito com o senhor. Obrigada.

Ao *Prof. Ass. Dr. Juliano Pelim Pessan*, pelas risadas, companheirismo, acessibilidade e todo empenho pelo seu trabalho, sou muito grata por toda contribuição que me proporcionaste.

Às excelentes funcionárias da seção de Pós-graduação da Faculdade de Odontologia de Araçatuba - UNESP, *Valéria, Cristiane e Lilian*, pelo apoio, suporte e ajuda a mim dispensados.

Aos queridos *Pós-graduandos* do Departamento de Odontopediatria da Faculdade de Odontologia de Araçatuba - UNESP, pelo convívio maravilhoso, pela amizade e por toda a ajuda. Graças a vocês me sinto em casa neste Departamento.

Ao meu amigo *Renan Aparecido Fernandes*, por toda a cumplicidade e amizade verdadeira. Eu agradeço muito a Deus por ter colocado você no meu caminho durante a graduação, e principalmente por você ainda fazer parte da minha vida não só acadêmica, mas também pessoal,

a minha consideração por você é enorme, obrigada por me ajudar e estar sempre do meu lado em todos os momentos. Amo você meu amigo.

A minha amiga *Laura Pires Barcelos*, mesmo com quilômetros de distância você nunca deixou de estar presente, a vida segue e a gente corre atrás dos nossos sonhos mas nós sempre vamos cumprir a promessa de estarmos aqui, uma pela outra. Obrigada por ser a minha amiga, a minha irmã, a minha fiel escudeira. Eu te amo muito.

A minha amiga *Ana Beatriz Repizo Renesto* que faz de Araçatuba um lugar muito melhor, obrigada por todos os momentos incríveis que passamos juntas, por cuidar de mim, por me ouvir, enfim obrigada por ser tão incrível, você com certeza foi um anjo que Deus enviou para a minha vida e que eu vou levar pra sempre. Eu amo muito você.

Ao meu amigo *Willian Henrique Jacometo*, você com certeza é o amigo mais justo e mais bondoso que eu tenho, eu te admiro muito e acredito no seu potencial, obrigada por se preocupar comigo e me dar a certeza de que eu posso sempre contar com você.

A minha amiga *Marina Migliorucci*, obrigada por ser tão especial, por me ajudar tanto em todos os sentidos sem medir esforços, por todos os momentos incríveis que passamos juntas, por me dar a certeza de que eu sempre posso confiar em você.

A minha amiga *Jackeline Gallo do Amaral*, obrigada não só pela imensa ajuda que você me deu em todo o desenvolvimento do mestrado, com certeza você foi a minha co-orientadora do coração, e

eu fico muito feliz que essa relação profissional tenha se tornado uma grande amizade, eu te admiro muito e acredito no seu futuro brilhante como professora e pesquisadora.

“Se as coisas são inatingíveis... ora!

Não é motivo para não querê-las.

Que tristes os caminhos, se não fora a presença distante das estrelas.”

Mario Quintana

Fernandes GL. **Nanopartículas de prata e glicerofosfato de cálcio: sínteses por rotas convencionais e fitoquímica, análise antimicrobiana e avaliação da citotoxicidade** [dissertação]. Araçatuba: Universidade Estadual Paulista; 2016.

RESUMO GERAL

O objetivo geral desse estudo foi sintetizar e caracterizar nanobiomateriais compostos por nanopartículas de prata (AgNP) e glicerofosfato de cálcio (CaGP) sintetizados por rotas químicas utilizando-se borihidreto de sódio ou citrato de sódio e fitoquímica por meio de extrato da casca de romã, e avaliar seu efeito antimicrobiano contra cepas de referência de *Candida albicans* (ATCC 10231) e *Streptococcus mutans* (ATCC 25175) e sua citotoxicidade em células de fibroblastos (L929). Além do agente redutor, para as sínteses químicas variou-se a concentração de prata (1 ou 10%), a apresentação do CaGP (micro ou nanoparticulado), o solvente utilizado na síntese (água deionizada ou isopropanol) e a forma dos nanocompostos (em suspensão, seco em estufa ou liofilizado). Para a síntese fitoquímica utilizou-se o extrato da casca desidrata da romã, obtido por percolação em etanol (70%) e com os compostos totais fenólicos expressos em ácido gálico e a concentração de ácido elágico quantificados respectivamente por método colorimétrico e HPLC. A caracterização dos nanocompostos e dos controles contendo somente AgNP foi feita por UV-Vis, MEV, e EDX. A ação antimicrobiana foi avaliada por meio da mínima contração inibitória de acordo com o método da microdiluição (CLSI M27-A2 e M07-A9), enquanto que a viabilidade celular dos fibroblastos foi quantificada utilizando-se método fluorimétrico (Alamar Blue). Esses experimentos foram realizados em triplicata em três ocasiões diferentes e os dados de porcentagem de viabilidade celular foram analisados pela ANOVA de um fator seguido do teste de Bonferroni ($\alpha=5\%$). Para todas as sínteses houve formação de AgNP associadas ao CaGP. Contudo pela microscopia somente na concentração de 10% de prata visualizou-se as AgNP decorando a superfície do CaGP (síntese com borihidreto de sódio e isopropanol) ou envolta pelo CaGP (síntese com borihidreto e água e com casca da romã). Os nanocompostos sintetizados quimicamente foram mais efetivos contra os microrganismos testados que os sintetizados pela rota fitoquímica, especialmente quando utilizou-se citrato de sódio como agente redutor. Pela rota fitoquímica com a romã, o nanocomposto AgNP-CaGP foi mais efetivo contra *C. albicans* que o controle AgNP e o contrário ocorreu para *S. mutans*. A utilização do extrato da romã para as sínteses reduziu significativamente ($p < 0,05$) a citotoxicidade tanto do nanocomposto AgNP-CaGP como das AgNP quando comparados com aqueles sintetizados quimicamente, independente do agente redutor utilizado na reação. Ainda, para todas as sínteses,

o CaGP reduziu significativamente ($p < 0,05$) a citotoxicidade dos nanocompostos AgNP-CaGP quando comparados com as AgNP isoladas. Conclui-se que os nanocomposto formado por AgNP e CaGP apresenta efetividade antimicrobiana contra importantes patógenos relacionados a cárie dentária e que sua citotoxicidade foi reduzida quando utilizou-se a casca da romã como agente redutor da prata.

Palavras-chave: Nanopartículas, Punicaceae, *Candida albicans*, *Streptococcus mutans*, Citotoxicidade celular

Fernandes GL. **Silver nanoparticles and calcium glycerophosphate: synthesis by conventional and phytochemical routes, antimicrobial analysis and evaluation of cytotoxicity** [dissertação]. Araçatuba: Universidade Estadual Paulista; 2016.

GENERAL ABSTRACT

The aim of this study was to synthesize and characterize nanomaterials compounds by silver nanoparticles (AgNP) and calcium glycerophosphate (CaGP) synthesized by chemical route using sodium borohidreto or sodium citrate, and phytochemical through pomegranate peel extract, and evaluate its antimicrobial effect against reference strains of *Candida albicans* (ATCC 10231) and *Streptococcus mutans* (ATCC 25175) and its cytotoxicity in fibroblast cells (L929). Besides, reducing agent for chemical syntheses, is varied the silver concentration (1 or 10%), the form of CAGP (micro or nanoparticulate), the solvent used in synthesis (deionized water or isopropanol) and the form of the nanocomposite (suspended, dry in incubator or lyophilized). For the phytochemical synthesis, utilized the peel extract of pomegranate obtained by percolation in ethanol (70%) and total phenolic compounds was expressed in gallic acid standard and ellagic acid concentration respectively quantified by colorimetric method HPLC. The characterization of nanocomposites and controls containing only AgNP was made by UV-Vis spectroscopy, SEM and EDX. The antimicrobial activity was evaluated by the minimum inhibitory concentration according to the microdilution method (CLSI M27-M07-A2 and A9), whereas fibroblast cell viability was quantitated using fluorimetric method (Alamar Blue). These experiments were performed in triplicate on three different occasions and the cell viability percentage data were analyzed by one-way ANOVA followed by Bonferroni test ($\alpha = 5\%$). For all syntheses were associated between AgNP and CaGP. However only by microscopy at a concentration of 10% silver visualized the AgNP decorating the surface of CaGP (synthesis with sodium borohidreto and isopropanol) shrouded by CaGP or (synthesis with borohidreto and water and pomegranate peel). The nanocompounds synthesized by chemical route, were more effective against the microorganisms than synthesized by the phytochemical route, especially when used sodium citrate as reducing agent. Through the phytochemical route with the pomegranate, the AgNP-CaGP nanocomposite was more effective against *C. albicans* than AgNP and the opposite occurred to *S. mutans*. The use of pomegranate extract for the synthesis significantly ($p < 0.05$) cytotoxicity both AgNP-CaGP nanocomposite of AgNP as compared to those synthesized chemically, regardless of the reducing agent used in the reaction. Yet, for all the syntheses, the CaGP reduced significantly ($p < 0.05$) the cytotoxicity of nanocomposites AgNP-CaGP when compared with the isolated AgNP. It concludes that the nanocomposite formed by AgNP and CaGP has antimicrobial effectiveness against important pathogens related with caries and their cytotoxicity was reduced when used the pomegranate peel as reducing agent of silver.

Keywords: Nanoparticles, Punicaceae, *Candida albicans*, *Streptococcus mutans*, Celular cytotoxicity

LISTA DE FIGURAS

Chapter 1	Calcium glycerophosphate impregnated with silver nanoparticles by sodium citrate and sodium borohydride route: Characterization and antimicrobial efficacy	28
Figure 1	a) UV–Visible spectrum and b) XRD pattern of Ag-CaGP (B4 group) nanocomposite, silver nanoparticles and CaGP.	45
Figure 2	SEM images of the Ag-CaGP nanocomposites: B4 (a and b), C4 (c and d) and B8 (e and f) in different magnifications. The arrows indicate silver nanoparticles on the surface of CaGP in B4 and in the bulk of CaGP in C4 and B8.	46
Figure 3	SEM and EDS mapping of the 2D elements issuance Si K α , O K α , P K α , Ca K α and Ag K α false color. Analysis of the distribution of silver nanoparticles on the Ag-CaGP for sample B4: a) SEM image; b) chemical mapping of silicon element present in the substrate, where the electron beam was focused directly on the substrate and is showed in green color, and the dark regions the beam was focused in Ag-CaGP nanocomposite B4; c-f) oxygen, calcium, phosphorus and silver, respectively, demonstrating they are constituents of the Ag-CaGP.	47
Figure 4	SEM and EDS mapping of the 2D elements issuance Si K α , O K α , P K α , Ca K α and Ag K α false color. Analysis of the distribution of silver nanoparticles on the Ag-CaGP for sample C4: a) SEM imge; b) chemical mapping of silicon element present in the substrate, where the electron beam was focused directly on the substrate and is showed in green color, and the dark regions the beam was focused in Ag-CaGP nanocomposite C4; c-f) oxygen, calcium, phosphorus and silver, respectively, demonstrating they are constituents of the Ag-CaGP.	48
Chapter 2	Synthesis, characterization and antimicrobial efficacy of a nanocomposite composed by calcium glycerophosphate and silver nanoparticles reduce by peel extrac of pomegranate	49
Figure 1	a) UV–Visible spectrum and b) XRD pattern of Ag-CaGP nanocomposite, silver nanoparticles and CaGP	72
Figure 2	SEM images (a and b) in different magnifications of the AgNP with size of approximately 50 nm and uniform distribution of this nanoparticles	73
Figure 3	SEM images (a and b) in different magnifications of the Ag-CaGP nanocomposite with silver nanoparticles on the surface of the CaGP: a-	74

b) silver nanoparticles showed in white little spheres dispersed on the CaGP bulk.

Figure 4	SEM and EDS mapping of the 2D elements issuance Si K α , O K α , P K α , Ca K α and Ag K α false color. Analysis of the distribution of silver nanoparticles on the Ag-CaGP a) SEM image; b) chemical mapping of silicon element present in the substrate, where the electron beam was focused directly on the substrate and is showed in green color, and the dark regions the beam was focused in Ag-CaGP nanocomposite; c-f) oxygen, calcium, phosphorus and silver, respectively, demonstrating they are constituents of the Ag-CaGP.	75
Chapter 3	Synthesis and characterization of nanocomposites composed by calcium glycerophosphate and silver nanoparticles reduced by chemical and green route and cytotoxicity activities	76
Figure 1	a) UV–Visible spectrum and b) XRD pattern samples Ag-CaGP/B; Ag CaGP/C; Ag-CaGP/E; AgNP/E and CaGP.	96
Figure 2	Figure 2. SEM images of the nanocompounds: a) Ag-CaGP/E; b) Ag CaGP/B; c) Ag-CaGP/C.	97
Figure 3	Cell Cytotoxicity obtained by Alamar Blue assay for compounds Ag-CaGP/E; Ag-CaGP/B; Ag-CaGP/C in L929 fibroblast cells. * Indicates statistical differences between the concentration tested and positive control (100% viable cells) and ** indicates statistical difference between the groups at the same concentration (Bonferroni, p <0.05).	98
Figure 4	Cell Cytotoxicity obtained by Alamar Blue assay for compounds Ag-CaGP/E; Ag-CaGP/B; Ag-CaGP/C in L929 fibroblast cells. * Indicates statistical differences between the concentration tested and positive control (100% viable cells) and bars indicates statistical difference between the groups at the same concentration (Bonferroni, p <0.05).	99
Figure 5	Cell Cytotoxicity obtained by Alamar Blue assay for controls in L929 fibroblast cells. * Indicates statistical differences between the concentration tested and positive control (100% viable cells) (Bonferroni, p <0.05)	100

LISTA DE TABELAS

Chapter 1	Calcium glycerophosphate impregnated with silver nanoparticles by sodium citrate and sodium borohydride route: Characterization and antimicrobial efficacy	28
Table 1	Minimum inhibitory concentrations (MIC) of %Ag/CaGP nanocomposites against microorganisms tested and silver ions concentrations.	44
Table 2	Minimum inhibitory concentrations (MIC) and silver ions concentration of control solutions.	44
Chapter 2	Synthesis, characterization and antimicrobial efficacy of a nanocomposite composed by calcium glycerophosphate and silver nanoparticles reduce by peel extract of pomegranate	49
Table 1	Minimum inhibitory concentrations (MIC) of green AgNP and Ag-CaGP, based on dry matter of the extract extract by percolation process, phenolic contents, elagic acid and silver concentration.	71
Chapter 3	Synthesis and characterization of nanocomposites composed by calcium glycerophosphate and silver nanoparticles reduced by chemical and green route and cytotoxicity activities	76
Table 1	Groups tested according to reducing agent, solvent and compounds used.	95

SUMÁRIO

Introdução Geral	20
Capítulo 1: Calcium glycerophosphate impregnated with silver nanoparticles by sodium citrate and sodium borohydride route: Characterization and antimicrobial efficacy	25
Abstract	26
Introduction	27
Materials and methods	29
Results	32
Discussion	34
References	38
Capítulo 2: Synthesis, characterization and antimicrobial efficacy of a nanocomposite composed by calcium glycerophosphate and silver nanoparticles reduced by peel extract of pomegranate	46
Abstract	47
Introduction	49
Materials and methods	52
Results and Discussion	57
References	63
Capítulo 3: Synthesis and characterization of nanocomposites composed by calcium glycerophosphate and silver nanoparticles reduced by chemical and green route and cytotoxicity activities	73
Abstract	74
Introduction	76
Materials and methods	78
Results	82
Discussion	84
References	88

Anexos	98

INTRODUÇÃO GERAL

1. INTRODUÇÃO GERAL

A nanotecnologia, uma das áreas mais emergentes [Hussain et al 2015] no campo da pesquisa, tem como objetivo a manipulação de partículas permitindo a síntese de novos materiais. [Zandparsa 2014]. Nesse contexto, o desenvolvimento e caracterizações desses biomateriais tem sido realizada [de Oliveira and Cardoso 2014] para a sua aplicabilidade em diversas áreas como a medicina e a odontologia [Zandparsa 2014].

Dentro da odontologia, uma das aplicações da nanotecnologia, é em alternativas de tratamento para a cárie dentária [Zandparsa 2014], uma das doenças mais comuns nos seres humanos caracterizada por uma destruição localizada e irreversível dos dentes [Metwali et al. 2013].

O *Streptococcus mutans*, devido a sua capacidade de produzir ácidos e glucanos, e de sobreviver em meios ácidos, é um dos principais microrganismos relacionados com a cárie dentária. Além do *S. mutans*, pesquisas recentes mostram a presença de *C. albicans* nos biofilmes orais, sugerindo uma interação entre esses microrganismos na patogenicidade da cárie [Metwalli et al. 2013].

A resistência antimicrobiana desses microrganismos em biofilmes a diversos antimicrobianos [Monteiro et al. 2011; Monteiro et al. 2009] faz com que as Nanopartículas de prata (AgNP) sejam pesquisadas como uma alternativa devido a sua aplicabilidade contra um amplo espectro de bactérias, fungos e vírus [Pérez-Díaz et al. 2015; Besinis et al. 2014; Li et al. 2008; Ge et al.2014; Wei et al. 2015; Kim et al. 2016].

Embora o mecanismo exato de ação das AgNP não seja exatamente compreendido, acredita-se que esteja relacionado a liberação de íons Ag a partir das AgNP [Kim et al. 2007; Besinis et al. 2014; Yang et al 2012], além da produção de um stress oxidativo nas células dos microrganismos devido a geração de espécies reativas de oxigênio (ROS)[Fu et al. 2014; Foldbjerg et al. 2011] que interagem com componentes citoplasmáticos e do DNA, inibindo enzimas da cadeia respiratória e alterando a permeabilidade da membrana citoplasmática [Damm et al. 2008; Panáček et al 2006; Monteiro et al. 2009; Azam et al 2012; Di Giulio et al 2013; Kim et al. 2009; Monteiro et al. 2012].

As AgNP podem ser sintetizadas por diferentes rotas, incluindo as rotas químicas convencionais e também rotas *green* [U.S.EPA 2012]. As vantagens da rota *green* incluem principalmente a utilização de materiais não tóxicos no processo de síntese, além disso os agentes redutores tendem a reduzir e estabilizar essas AgNP [Amooaghaie et al. 2015; Park et al. 2014]. Isso se torna uma alternativa interessante uma vez que alguns autores mostraram que as AgNP podem ser tóxicas para as células humanas [Barbosa et al. 2014]. e essa toxicidade está relacionada com inúmeros fatores, dentre eles o tamanho, a dose, e os componentes envolvidos na síntese.[Ray et al 2009].

Vários produtos como os extratos de algumas plantas apresentam a capacidade de reduzir íons prata [Park et al. 2011]. Estudos mostram que os compostos fenólicos presentes nos extratos são responsáveis por essa redução. Nesse contexto, a *Punica granatum* se torna uma alternativa devido a sua composição rica em polifenóis e elagitanos como ácido elágico, punicalagina, ácido gálico entre outros [Ahmad et al. 2012; Heber 2011], que fazem com que essa fruta apresente características antioxidantes e anti-inflamatórias [Heber 2011; Henning 2011].

Não só a utilização de diversas rotas para a síntese das AgNP, mas pensando na sua aplicabilidade antimicrobiana, o desenvolvimento de um biomaterial associando essas nanopartículas com outros compostos se torna interessante. A associação com o Glicerofosfato de cálcio (CaGP), um sal de fosfato orgânico, contribuiria para o desenvolvimento de um biomaterial com propriedades anti-cáries, [do Amaral et al. 2013; Zaze et al. 2014; Lynch 2004; Nakashima 2009], uma vez que trabalhos na literatura mostraram que o CaGP apresenta uma interação direta com o esmalte do dente, reduzindo os efeitos do ácido, além de produzir um efeito tampão no pH do biofilme, elevando os níveis de cálcio e fósforo [Lynch 2004; Nakashima 2009].

Portanto, o objetivo geral dessa pesquisa foi sintetizar um biomaterial composto por AgNP (sintetizadas por rotas química e *green*) e CaGP, avaliar o seu efeito antimicrobiano contra cepas de

C. albicans ATCC 10231 e *S. mutans* ATCC 25175, além da toxicidade celular desse biomaterial contra fibroblastos L929.

References:

1. Ahmad N, Sharma S, Rai R. Rapid green synthesis of silver and gold nanoparticles using peels of *Punica granatum*. *Advanced Materials Letters*. 2012. Vol. 3:376-380.
2. Amooaghaie R, Saeri MR, Azizi M. Synthesis, characterization and biocompatibility of silver nanoparticles synthesized from *Nigella sativa* leaf extract in comparison with chemical silver nanoparticles. *Ecotoxicol Environ Saf*. 2015. Vol. 120:400-408.
3. Azam A, Ahmed AS, Oves M, Khan MS, Habib SS, Memic A. Antimicrobial activity of metal oxide nanoparticles against Gram-positive and Gram-negative bacteria: a comparative study. *Int J Nanomedicine*. 2012. Vol. 7:6003-6009.
4. Barbosa DB, Monteiro DR, Satie A, Gorup LF, Delbem ACB, Pessan JP, Camargo ER, Agostinho AM et al. 2014. *Encyclopedia of Biomedical Polymers and Polymeric Biomaterials*. Doi: 10.1081 IE-EBPP- 120051066
5. Besinis A, De Peralta T, Handy RD. The antibacterial effects of silver, titanium dioxide and silica dioxide nanoparticle compared to the dental disinfectant chlorhexidine on *Streptococcus mutans* using a suite of bioassays. *Nanotoxicology*. 2014. Vol. 8:1-16.
6. Damm C, Münstedt H, Rösch A. The antimicrobial efficacy of polyamide 6/silver-nano- and microcomposites. *Materials Chemistry and Physics*. 2008. Vol. 108: 61-66.
7. de Oliveira JF, Cardoso MB. Partial aggregation of silver nanoparticles induced by capping and reducing agents competition. *Langmuir*. 2014. Vol. 6:4879-4886.
8. Di Giulio M, Di Bartolomeo S, Di Campli E, Sancilio S, Marsich E, Travan A, Cataldi A, Cellini L. The effect of a silver nanoparticle polyssaccharide system on streptococcal and saliva-derived biofilm. *Int J Mol Sci*. 2013. Vol. 28 28:13615-13625.
9. do Amaral JG , Sasaki KT, Martinhon CC, Delbem AC. Effect of low-fluoride dentifrices supplemented with calcium glycerophosphate on enamel demineralization in situ. *Am J Dent*. 2013. Vol26:75-80.
10. Foldbjerg R, Dang DA, Autrup H. Cytotoxicity and genotoxicity of silver nanoparticles in the human lung cancer cell line, A549. . *Inorganic Compounds Archives of Toxicology*. 2011. Vol 85: 743-750.
11. Fu PP, Xia Q, Hwang HM, Ray PC, Yu H. Mechanisms of nanotoxicity: Generation of reactive oxygen species. *Journal of Food and Drug Analysis*. 2014. Vol 22: 64-75.
12. Ge L, Li Q, Wang M, Ouyang J, Li X, Xing MM. Nanosilver particles in medical applications: synthesis, performance, and toxicity. *International Journal Nanomedicine*. 2014. Vol. 9:2399-2407.
13. Heber D. Pomegranate Ellagitannins. *Herbal Medicine: Biomolecular and Clinical Aspects*. 2nd edition. 2011.
14. Henning SM, Zhang Y, Seeram NP, Lee RP, Wang P, Bowerman S, Heber D. Antioxidant capacity and phytochemical content of herbs and spices in dry, fresh and blended herb paste form. *International Journal of Food Sciences and Nutrition*. 2011. Vol. 62: 219-225.
1. Hussain I, Singh NB, Singh A, Singh H, Singh SC. Green synthesis of nanoparticles and its potential application. *Biotechnology Lett*. 2015:1-16
15. Kim JS, Kuk E, Yu KN, Kim JH, Park SJ, Lee HJ, Kim SH, Park YK, Park YH, Hwang CY, Lim YK, Lee YS, Jeong DH, Cho MH. Antimicrobial effects of silver nanoparticles. *Nanomedicine*. 2007. Vol3:95-101.
16. Kim KJ, Sung WS, Suh BK, Moon SK, Choi JS, Kim JG, Lee DG. Antifungal activity and mode of action of silver nanoparticles on *Candida albicans*. *Biometals*. 2009. Vol. 22:235-242.
17. Kim TY, Cha SH, Cho S, Park Y. Tannic acid-mediated green synthesis of antibacterial silver nanoparticles. *Arch. Pharm. Res*. 2016.
18. Li Q, Mahendra S, Lyon DY, Brunet L, Liga MV, Li D, Alvarez Pj. Antimicrobial nanomaterials for water disinfection and microbial control: potential application and

- implications. *Water Res.* 2008. Vol. 42:4591-4602.
19. Lynch RJ. Calcium glycerophosphate and caries: a review of the literature. *Int Dent J.* 2004. Vol. 54:310-314.
 20. Metwalli KH, Khan SA, Krom BP, Jabra-Rizk MA. *Streptococcus mutans*, *Candida albicans*, and the human mouth: a sticky situation. *PloS Pathog.* 2013. Vol. 9:e1003616.
 21. Monteiro DR, Gorup LF, Silva S, Negri M, de Camargo ER, Oliveira R, Barbosa DB, Henriques M. Silver colloidal nanoparticles: antifungal effect against adhered cells and biofilms of *Candida albicans* and *Candida glabrata*. *Biofouling*, 2011. Vol. 27:711-719.
 22. Monteiro DR, Gorup LF, Takamiya AS, Ruvollo-Filho AC, de Camargo ER, Barbosa DB. The growing importance of materials that prevent microbial adhesion: antimicrobial effect of medical devices containing silver. *Int J Antimicrob Agents.* 2009. Vol. 34:103-110.
 23. Monteiro DR, Silva S, Negri M, Gorup LF, de Camargo ER, Oliveira R, Barbosa DB, Henriques M. Silver nanoparticle: influence of stabilizing agent and diameter on antifungal activity against *Candida albicans* and *Candida glabrata* biofilms. *Lett Appl Microbiol.* 2012. Vol. 54:383-391.
 24. Nakashima S, Yoshie M, Sano H, Bahar A. Effect of a test dentifrice containing nano-sized calcium carbonate on remineralization of enamel lesions in vitro. *Journal of Oral Science.* 2009. Vol.51:69-77.
 25. Panáček A, Kvítek L, Pucek R. Silver colloid nanoparticles: synthesis, characterization, and their antibacterial activity. *Journal of Physical Chemistry B*, 2006. Vol. 110: 16248-16253
 26. Park Y, Hong YN, Weyers A, kim YS, Linhardt RJ. Polysaccharides and phytochemicals: a natural reservoir for the green synthesis of gold and silver nanoparticles. *IET Nanobiotechnology.* 2011. Vol. 5: 69-78.
 27. Park Y. A new paradigm shift for the green synthesis of antibacterial silver nanoparticles utilizing plant extracts. *Toxicol.* 2014. Vol. 30:169-178
 28. Pérez-Díaz MA, Boegli L, James G, Velasquillo C, Sánchez-Sánchez R, Martínez-Martínez RE, Martínez-Castañón GA, Martínez-Gutierrez F. Silver nanoparticles with antimicrobial activities against *Streptococcus mutans* and their cytotoxic effect. *Mater Sci Eng C Mater Biol Appl.* 2015. Vol. 55:360-366.
 29. Ray PC, Yu H, Fu PP. Toxicity and Environmental Risks of Nanomaterials: Challenges and Future Needs. *Journal of Environmental Science and Health, Part C Environmental Carcinogenesis and Ecotoxicology Reviews.* 2009. Vol. 27:1-35.
 30. Wei L, Lu J, Xu H, Patel A, Chen ZS, Chen G. Silver nanoparticles: synthesis, properties, and therapeutic applications. *Drug Discov Today.* 2015. Vol 20:595-601.
 31. Yang X, Gondikas AP, Marinakos SM, Auffan M, Liu J, Kim HH. Mechanism of silver nanoparticle toxicity is dependent on dissolved silver and surface coating in *Caenorhabditis elegans*. *Environmental Science & Technology.* 2012. Vol. 46: 1119-1127.
 32. Zandparsa R. Latest biomaterials and technology in dentistry. *Dent Clin North Am.* 2014. Vol. 58:113-134.
 33. Zaze AC, Dias AP, Amaral JG, Miyasaki ML, Sasaki KT, Delbem AC. In situ evaluation of low-fluoride toothpastes associated to calcium glycerophosphate on enamel remineralization. *J Dent.* 2014. Vol.42:1621-1625.

CAPÍTULO 1

Calcium glycerophosphate impregnated with silver nanoparticles by sodium citrate and sodium borohydride route: Characterization and antimicrobial efficacy .

Calcium glycerophosphate impregnated with silver nanoparticles by sodium citrate and sodium borohydride route: Characterization and antimicrobial efficacy

Abstract

The aim of this study was to synthesize and characterize a biomaterial containing silver nanoparticles (Ag) and calcium glycerophosphate (CaGP) (Ag/CaGP) using sodium borohydride (NaBH_4) or sodium citrate ($\text{Na}_3\text{C}_6\text{H}_5\text{O}_7$) as reducing agent. Its antimicrobial activity was evaluated by microdilution broth method (Minimum inhibitory concentration, MIC) against reference strains of *Candida albicans* (ATCC 10231) and *Streptococcus mutans* (ATCC 25175). Synthesis were performed using silver nitrate (1 or 10%), NaBH_4 or $\text{Na}_3\text{C}_6\text{H}_5\text{O}_7$, CaGP (commercial or nanoparticulated), ammonium salt of methacrylic poly acid polymer and deionized water or isopropanol as solvent. Ag/CaGP was characterized by X-ray diffraction, scanning electron microscopy and mapping in 2D by EDX, UV-Vis spectroscopy. The results indicated the formation of Ag nanoparticles associated with CaGP, regardless of the Ag concentration and the type of CaGP. Ag/CaGP reduced by $\text{Na}_3\text{C}_6\text{H}_5\text{O}_7$ was effective against *C. albicans* (1%-commercial and -nanoparticulated: 156.2 to 312.5 $\mu\text{g/mL}$; 10%-commercial: 39.05 $\mu\text{g/mL}$ and nanoparticulated: 19.5 to 39.05 $\mu\text{g/mL}$) and *S. mutans* (1%-commercial and -nanoparticulated: 1250 $\mu\text{g/mL}$; 10%-commercial: 312.5 to 625 $\mu\text{g/mL}$ and -nanoparticulated: 156.2 to 312.5 $\mu\text{g/mL}$). While by NaBH_4 route the MIC values were found only for *C. albicans* using isopropanol as solvent (1%-commercial: was not effective and -nanoparticulated: 400-800 $\mu\text{g/mL}$; 10%- commercial: 400-1600 $\mu\text{g/mL}$ and -nanoparticulated: 100-200 $\mu\text{g/mL}$). In conclusion, the synthesis proposed promoted the anchorage of silver nanoparticles on the surface of the CaGP, and the nanocomposites produced using $\text{Na}_3\text{C}_6\text{H}_5\text{O}_7$ were effective against both microorganisms tested.

Key-words: Silver; calcium glycerophosphate; nanoparticles; *Streptococcus mutans*; *Candida albicans*

Introduction

The synthesis and study of properties of new biomaterials has been lately emphasized with the improvement of nanotechnology. In this context, the development of nanomaterials has been the focus of many areas of chemistry, physics and materials science because of the promising characteristics that these materials exhibit [1].

Nanotechnology aims to manipulate particles by creating new structures with favorable properties in many areas such as medicine and dentistry [2], and new alternatives of treatment for oral pathologies are emerging. Metallic nanoparticles, in particular silver nanoparticles (AgNP), have been studied as an alternative antimicrobial agent against a broad spectrum of species in the control of oral biofilms [3-5]. Although there are several studies where AgNP are used as antimicrobial agents, their mechanism of action is not completely understood. Kim et al. [6] and Besinis et al. [4] related their antimicrobial action to the toxicity resulting from free metal ions dissolution from the surface of the AgNP. In addition, AgNP would lead to oxidative stress through the generation of reactive oxygen species (ROS), interacting with cytoplasmic and nucleic acid components by inhibiting enzymes of the respiratory chain and changing the permeability of cytoplasmic bacterial membrane [6; 11-14].

Among oral pathologies, dental caries is one of the most common diseases in humans which relates to genetics, saliva, and diet of the host [12]. *Streptococcus mutans* is the main cariogenic microorganism owing its ability to produce acids and glucans from sugar metabolism which exceed the buffering capacity of saliva [12-14] and leads by a localized and irreversible destruction of the tooth structure [12;15]. However, recent evidence indicates the presence of *C. albicans* and *S. mutans* in oral biofilms, suggesting that the interaction between them can lead to the development of caries [12;16;17]. *C. albicans* colonization depends on the presence of the bacteria which besides promoting adhesion sites, act as a carbon source for yeast growth. On the other hand, yeasts reduce the levels of oxygen for streptococci [12;18]. Studies have shown the resistance of many

microorganisms to antimicrobial agents currently used [7;19]

Thinking of favoring the remineralization process in dental caries, calcium phosphate derivatives have been reported since of 1930 [20]. Calcium glycerophosphate (CaGP) is an organic phosphate salt with anti-caries properties demonstrated in studies carried out in monkeys [21] and in rats [22]. Its action in dental biofilms may be related to the increase of calcium and phosphate levels [23], buffering capacity [21] and reduction of the mass of the biofilms [24]. Because it seems to interact with dental tissues [25], CaGP has been incorporated in dentifrices [26-27]. Amaral et al. [28] and Zaze et al. [29] when associated CaGP (0.25%) in toothpastes with fluoride at low concentration found the same efficacy against caries in enamel when compared to dentifrices supplemented with higher concentration of fluoride demonstrating CaGP be an good option for oral products to both prevent caries and avoid fluorose in dental tissues.

The use of a biomaterial containing both an antimicrobial and a compound acting as a source of calcium phosphate for dental remineralization would have a great impact on the prevention and control of dental caries. Therefore, this study aimed to synthesize a nanobiomaterial containing CaGP and AgNP using two different reducing agents, sodium borohydride or sodium citrate, and subsequently evaluate their antimicrobial activity against ATCC strains of *Candida albicans* and *Streptococcus mutans*.

Materials and Methods

Synthesis of silver-calcium glycerophosphate (Ag-CaGP) nanocomposites

Ag-CaGP nanocomposites were synthesized at the Interdisciplinary Laboratory of Electrochemistry and Ceramics of the Chemistry Department in Federal University of São Carlos. Initially, the commercial form of calcium glycerophosphate (80% β -isomer and 20% rac- α -isomer, CAS 58409-70-4, Sigma-Aldrich Chemical Co, St Louis, Missouri, USA) was acquired and was nanoparticulated using a ball mill for 24 hours at 120 rpm, obtaining nanoparticles of approximately 10 nm. Then, two chemistry methods were employed for the synthesis. The first method employed as reducing agent the sodium borohydride (NaBH_4 , Sigma-Aldrich Chemical Co, St Louis, Missouri, USA) and was based on the methodology proposed by Miranda et al. [30]. The synthesis was carried out in an alcoholic medium (isopropanol) or deionized water. For this, suspensions containing 5g of CaGP and silver nitrate (AgNO_3 Merck KGaA, Darmstadt, Hessen, Germany) at 0.85 or 0.085 g were prepared in the presence of 0.5 mL of a surfactant (ammonium salt of polymethacrylic acid (NH-PM), Polysciences Inc., Warrington, PA, USA) (Table 1). Then, NaBH_4 (0.015 g) was added to each suspension, which caused the reduction of Ag^+ to metallic silver nanoparticles in the presence of CaGP. The molar stoichiometric ratio between Ag^+ and NaBH_4 was 1:1.26, respectively. The second method was based on the proposed by Turkevich et al. [33] and Gorup et al. [34]. The reducing agent of AgNO_3 was sodium citrate ($\text{Na}_3\text{C}_6\text{H}_5\text{O}_7$, Merck KGaA) and the stoichiometric ratio of each compound was respectively 1:3. Thus, in a flask containing 100 mL of deionized H_2O 5g of CaGP was added following of 0.5 mL NH-PM and 1.4 g of $\text{Na}_3\text{C}_6\text{H}_5\text{O}_7$. This mixture was kept under magnetic stirring and heating. After reaching 95°C temperature AgNO_3 was added and this suspension was maintained stirring for 30 minutes until occurring the color change, which qualitatively indicated the formation of AgNP. Controls containing only the reducing agents and surfactant, and AgNP produced by both reducing were also prepared.

Characterization of Ag-CaGP nanocomposites

In order to demonstrate the presence of AgNP and CaGP in the compounds, the UV-Vis absorption spectroscopy was employed. The measure is based on the phenomenon of plasmon resonance band, observed in metallic nanoparticles. Thus, UV-Vis spectra of Ag-CaGP nanocomposites were obtained from aqueous solutions poured out in a commercial quartz cuvette with 1 cm optical path using a spectrophotometer (Shimadzu MultSpec-1501 spectrophotometer; Shimadzu Corporation, Tokyo, Japan) at 300 to 800 nm. Water was used as blank.

After a drying step, the resulting powder Ag-CaGP was subjected to X-ray diffraction (XRD) phase characterization using Cu K α radiation ($\lambda = 1.5406 \text{ \AA}$), generated at a voltage of 30 kV and a current of 30 mA with continuous sweep in the range of $5 < 2\theta < 80^\circ$, at scan rate of $2^\circ/\text{min}$ (Diffractometer Rigaku DMax-2000PC, Rigaku Corporation, Tokyo, Japan). The particles morphology was also characterized by scanning electron microscopy (SEM) on a Zeiss Supra 35VP microscope (S-360 microscope, Leo, Cambridge, USA) with field emission gun electron effect (FEG-SEM) operating at 10 kV. A drop of each sample were added with a micropipette and deposited on silicon metal plate (111) and dried at 40°C for 2 hours. The contacts between the sample and the support were carried out with conductive silver ink. It was also performed EDX (Energy Dispersive X-Ray Detector) analyzes with mapping in 2D. 2D images were constructed by analyzing energy released from the emission Si K α , O K α , P K α , Ag L α_1 e Ca K α . At the images, it is attributed false color to highlight the silver and for oxygen, silicon, phosphate and calcium.

Minimum inhibitory concentration (MIC)

The MIC tests were performed using the microdilution method according to the Clinical Laboratory Standards Institute guidelines for *Candida albicans* (M27-A2) and *Streptococcus mutans* (M07-A9), which were obtained from American Type Culture Collection (ATCC). *Candida albicans* (ATCC 10231) was cultivated on Sabouraud Dextrose Agar (SDA, Difco) media and *S. mutans*

(ATCC 25175) on Brain Heart Infusion Agar (BHI, Difco, Le Pont de Claix, France). Inocula from 24 h cultures on the respective media were adjusted to a turbidity equivalent to a 0.5 McFarland standard in saline solution (0.85% NaCl). This suspension was diluted (1:5) in saline solution and afterwards diluted (1:20) in RPMI 1640 (Sigma-Aldrich) or BHI. Initially, the Ag-CaGP nanocomposite was diluted in deionized water in a geometric progression, from 2 to 1024 times. Afterwards, each Ag-CaGP nanocomposite concentration obtained previously was diluted (1:5) in RPMI 1640 medium for *C. albicans* and in BHI for *S. mutans*. The final concentrations of Ag-CaGP nanocomposite in the dispersion ranged from 5 mg/mL to 0.01 mg/mL. Each inoculum (100 μ L) was added to the respective well of microtiter plates containing 100 μ L of each specific concentration of Ag-CaGP nanocomposite solution. The microtiter plates were incubated at 37°C, and the MIC values were determined visually as the lowest concentration of Ag-CaGP with no microorganism growth after 48 h for *C. albicans* and 24 h for *S. mutans*. All assays were repeated in triplicate on three different occasions.

Determination of Ag⁺ concentration

The evaluation of Ag⁺ concentration in AgCaGP and AgNP obtained by both reducing agents was determined by a specific electrode 9616 BNWP (Thermo Scientific, Beverly, MA, USA) coupled to an ion analyzer (Orion 720 A⁺, Thermo Scientific, Beverly, MA, USA). A 1000 μ g/mL silver standard was prepared placing 1.57 g of dried AgNO₃ into a 1 L volumetric flask containing deionized water. This solution was stored in an opaque bottle in a dark location and diluted in deionized water at the moment of dosage in order to achieve the standard concentrations used. Thus, the combined electrode was calibrated with standards containing 6.25 to 100 μ g Ag/ml at the same conditions of samples. A silver ionic strength adjuster solution (ISA, Cat. No. 940011) which provides a constant background ionic strength was used (1 mL of each sample/standard: 0.02 mL ISA).

Results

Synthesis and characterization of Ag-CaGP nanocomposites

UV-Vis absorption spectroscopy showed Ag-CaGP nanocomposites presented silver in nanosized dimensions in all nanocomposites synthesized, regardless of the reducing agent used. It was demonstrated by the presence of an intense absorption peak, denominated plasmonic band, which occurred between 420 and 450 nm (Figure 1a). It characterizes noble metal nanoparticles, with strong absorption band observed in the visible region [35]. The CaGP did not exhibit absorption peak in the visible region of the electromagnetic spectrum.

XRD pattern indicated that all Ag-CaGP nanocomposites were composed of AgNP and CaGP for confirming the presence of silver in Ag-CaGP nanocomposites through comparison of the nanoparticles and CaGP. The typical powder XRD pattern of the prepared CaGP showed diffraction peaks at $2\theta = 6.30^\circ, 12.3^\circ, 26.4^\circ, 41.1^\circ, \text{ and } 44.2^\circ$ (Figure 1b) and the corresponding crystallographic form (PDF № 1-17) [36]. The typical powder XRD pattern of the silver nanoparticles showed (Figure 1b) diffraction peaks at $2\theta = 38.2^\circ, 44.4^\circ, 64.6^\circ, 77.5^\circ, \text{ and } 81.7^\circ$, which can be indexed to (111), (200), (220), (311), and (222) planes of pure silver with face-centered cubic system (PDF № 04-0783).

SEM analyses showed spherical silver nanoparticles decorating the surface of the microparticles of CaGP without a definite shape, in all nanocomposites synthesized containing Ag at 10%. It was possible to observe the formation of silver nanoparticles anchored on the surface of CaGP (Figures 2).

The EDS showed clearly the outline of Ag-CaGP nanocomposites in all micrographies. Also, Figure 3 and 4 the 2D images were constructed by analyzing the energy released from the issuance Si $K\alpha$, O $K\alpha$, P $K\alpha$, Ca $K\alpha$ and Ag $K\alpha$, indicating the distribution of these elements on the demarcated area in the micrograph.

Minimum inhibitory concentration (MIC)

The results showed that the MIC values were related to the synthesis process and the Ag concentration used (Table 1). Nanocomposites obtained using $\text{Na}_3\text{C}_6\text{H}_5\text{O}_7$ as reducing agent showed the most effective antimicrobial activity against *C. albicans* and *S. mutans*. In these composites the lowest MIC values were observed for those containing 10% of Ag (C3 and C4), being between 19.05 and 39.05 $\mu\text{g}/\text{mL}$ for *C. albicans* and 156.2 and 625 $\mu\text{g}/\text{mL}$ for *S. mutans*. The nanocomposites synthesized using NaBH_4 as reducing agent and isopropanol as solvent showed fungicidal effect varying between 100 and 1600 $\mu\text{g}/\text{mL}$ as whilst no effect against *S. mutans* was observed. While the nanocomposites synthesized using the same reducing agent and deionized water as solvent did not show any effect against both microorganisms. The control solutions without silver and CaGP did not reveal any antimicrobial effect, as well as CaGP in the commercial and nanoparticulated form (Table 2).

Determination of Ag^+ concentration

The Ag^+ concentration of all nanocomposites containing Ag (AgNP and Ag-CaGP) is showed in Table 1. For samples obtained through NaBH_4 route (B1-B8) a reduction of ionic silver higher than 98% was observed, considering the total amount of ionic silver added to the reaction was 500 $\mu\text{g Ag}^+/\text{mL}$ for B1, B2, B5, B6 and 5000 $\mu\text{g Ag}^+/\text{mL}$ for B3, B4, B7 and B8. In spite of be observed a higher concentration of ionic silver for the compounds synthesized using $\text{Na}_3\text{C}_6\text{H}_5\text{O}_7$ as reducing agent, samples containing silver at 10% (C3 and C4) considering the total Ag^+ added to the reaction (5000 $\mu\text{g Ag}^+/\text{mL}$) presented $\geq 90\%$ of the ionic silver was reduced in these samples. C1 and C2 presented 61.1 and 33.3% respectively of ionic silver in samples as the total Ag^+ added in the reaction was 500 $\mu\text{g Ag}^+/\text{mL}$. For AgNP with no CaGP added to the reaction (Table 2) obtained by $\text{Na}_3\text{C}_6\text{H}_5\text{O}_7$ route (nanoAg($\text{Na}_3\text{C}_6\text{H}_5\text{O}_7$)) the Ag^+ concentration was 107.25 $\mu\text{g}/\text{mL}$, whereas for AgNP produced through NaBH_4 (nanoAg(NaBH_4)) the Ag^+ concentration was 576.19 $\mu\text{g}/\text{mL}$.

Discussion

In the present study, both synthesis methods proposed using sodium citrate or sodium borohydride as reducing agents, led the anchorage between the silver nanoparticles and calcium glycerophosphate (Figure 2). Besides, in general, the nanocomposites were effective against *Candida albicans* ATCC 10231 and/or *Streptococcus mutans* ATCC 25175. Showing that, this association doesn't interposed in the antimicrobial silver effectiveness, as it was observed for some authors studying Ag associated with hydroxyapatite [30-33].

Although the CaGP has been previously nanoparticulated before the Ag-CaGP synthesis, in our study it was not characterized as being in nanoparticulated form when associated with silver. It might be happen due to the poor solubility of calcium at pH=7 [30], even using the same dispersant (NH-PM) preconized by Miranda et al. [30]. A pastier bulk was particularly noted in micrographics of Ag-CaGP when water was used as solvent instead of isopropanol (Figure 2: c-f). Nevertheless, it did not interfere on the antimicrobial activity of Ag-CaGP synthesized through sodium citrate in which water was used as solvent for all synthesis. On the other hand, when sodium borohydride was used, water can have interfered in some way in the Ag-CaGP since the nanocompounds had no antimicrobial effect against both *C. albicans* and *S. mutans*, regardless of the silver concentration tested (1 or 10%). Moreover, considering the reducing agents, when sodium borohydride was employed, the silver nanoparticles showed the size between 10 to 40 nm, while using sodium citrate they were about 35 to 50 nm. The sodium borohydride seems to be a faster reducing agent than sodium citrate in AgNP synthesis process [37], in our study the reaction using it required longer time and higher temperature to reduce the silver ions from AgNO₃. Furthermore, the remain of silver ions in the synthesis must be considered, once several authors report that these ions are also responsible for the antimicrobial effect of AgNP [4; 38-41]. Thinking about it, the quantification of ions was accomplished using a silver electrode and it was observed that the C1-C4 synthesis feature larger amount of ions (Table 1).

However, it is possible that the silver nanoparticles present in the solution and also those associated with CaGP were responsible for the antimicrobial effect of the Ag-CaGP. Silver nanoparticles present a high reactive surface which tend to interact with sulfur groups from the cell membrane [38] as well as from sulfur-containing proteins in the interior of the bacterial cell and with phosphorus from DNA [38;42]. Moreover, as the charge of the membrane cell of bacteria at biological pH is negative due to the carboxylic groups [43;44], there would be an electrostatic force attraction leading to the nanoparticles to remain tightly bound to the bacteria [43]. Another interesting data in this study is that when CaGP was associated with silver nanoparticles the MIC values were lower than the values of silver nanoparticles without it was tested against *S. mutans* (Table 1). The CaGP might act as a buffer and likely would alter the charge of the *S. mutans* membrane and then improve the antibacterial effect of the nanocomposite Ag-CaGP [43;45;46]. It was also observed for *C. albicans*, where the addition of CaGP reduced the MIC values regardless of the reducing agent used.

Interesting, the Ag-CaGP nanocomposites were more effective against *C. albicans* than *S. mutans*. Although fungi are eukaryotes and their membranes are structurally different from bacterial cells, both present as the main component phospholipids, that contain phosphates groups which may be the target of the silver nanoparticles [47;48]. The results showed that not only the silver concentration in the Ag-CaGP (1 or 10%) interfered in their effect against *C. albicans* and *S. mutans* but the form of CaGP (micro or nanoparticulated), the solvent used, and the presence of ions also affected the MIC values. The past bulk formed when water was used as a solvent in the B4-B8 synthesis can interfere with the release of silver nanoparticles associated with the CaGP and consequently negatively influencing the antimicrobial effectiveness of these synthesis. Already in C1-C4, although water has been used as a solvent, the presence of ions may be responsible for the MIC results obtained against *C. albicans* and *S. mutans* and may suggest that the ions have an important role in *S. mutans*.

It is believed that the antifungal effect of the silver nanoparticles is related by disturbing the membrane potential caused the formation of pores and loss of intracellular components, causing cellular apoptosis [10;48-50]. Lara et al. [48] evaluated structural effects in *C. albicans* when subjected to silver nanoparticles in a very low concentration (0.0089 µg/mL) and demonstrated that silver nanoparticles damaged the inner layers of the cell wall increasing their permeabilization allowing the passage of these particles and consequently the disruption of the *C. albicans* cell membrane.

In conclusion, the synthesis proposed in this study promoted the anchorage of silver nanoparticles on the CaGP, and the nanocomposites produced using sodium citrate as reducing agent were effective against both microorganisms tested. Also, the highlight data found was that the addition of that phosphate with silver nanoparticles reduced the MIC values when compared with the MIC of silver nanoparticles by itself. So this study has been the beginning of others which goal in the future might be othe development of dental materials to not only control the growth of cariogenic microorganisms but also reduce the dentin/enamel demineralization.

Acknowledgements:

This study was supported by: São Paulo Research Foundation (FAPESP, Process 2013/24200-9 and 2014/08648-2), Brazil; and Coordination for the Improvement of Higher Education Personnel (Capes, Process 88887.068358/2014-00 and 88881.030445/2013-01), Brazil.

References:

1. de Oliveira JF, Cardoso MB. Partial aggregation of silver nanoparticles induced by capping and reducing agents competition. *Langmuir*. 2014. Vol. 6:4879-4886.
2. Latest biomaterials and technology in dentistry. *Dent Clin North Am*. 2014. Vol. 58:113-134.
3. Pérez-Díaz MA, Boegli L, James G, Velasquillo C, Sánchez-Sánchez R, Martínez-Martínez RE, Martínez-Castañón GA, Martínez-Gutierrez F. Silver nanoparticles with antimicrobial activities against *Streptococcus mutans* and their cytotoxic effect. *Mater Sci Eng C Mater Biol Appl*. 2015. Vol. 55:360-366.
4. Besinis A, De Peralta T, Handy RD. The antibacterial effects of silver, titanium dioxide and sílica dioxide nanoparticle compared to the dental disinfectant chlorhexidine on *Streptococcus mutans* using a suite of bioassays. *Nanotoxicology*. 2014. Vol. 8:1-16.
5. Li Q, Mahendra S, Lyon DY, Brunet L, Liga MV, Li D, Alvarez Pj. Antimicrobial nanomaterials for water disinfection and microbial control: potential application and implications. *Water Res*. 2008. Vol. 42:4591-4602.
6. Kim JS, Kuk E, Yu KN, Kim JH, Park SJ, Lee HJ, Kim SH, Park YK, Park YH, Hwang CY, Lim YK, Lee YS, Jeong DH, Cho MH. Antimicrobial effects of silver nanoparticles. *Nanomedicine*. 2007. Vol.3:95-101.
7. Monteiro DR, Gorup LF, Takamiya AS, Ruvollo-Filho AC, de Camargo ER, Barbosa DB. The growing importance of materials that prevent microbial adhesion: antimicrobial effect of medical devices containing silver. *Int J Antimicrob Agents*. 2009. Vol. 34:103-110.
8. Azam A, Ahmed AS, Oves M, Khan MS, Habib SS, Memic A. Antimicrobial activity of metal oxide nanoparticles against Gram-positive and Gram-negative bacteria: a comparative study. *Int J Nanomedicine*. 2012. Vol. 7:6003-6009.
9. Di Giulio M, Di Bartolomeo S, Di Campli E, Sancilio S, Marsich E, Travan A, Cataldi A, Cellini L. The effect of a silver nanoparticle polyssaccharide system on streptococcal and saliva-derived biofilm. *Int J Mol Sci*. 2013. Vol. 28 28:13615-13625.
10. Kim KJ, Sung WS, Suh BK, Moon SK, Choi JS, Kim JG, Lee DG. Antifungal activity and mode of action of silver nanoparticles on *Candida albicans*. *Biometals*. 2009. Vol. 22:235-242.
11. Monteiro DR, Silva S, Negri M, Gorup LF, de Camargo ER, Oliveira R, Barbosa DB, Henriques M. Silver nanoparticle: influence of stabilizing agent and diameter on antifungal activity against *Candida albicans* and *Candida glabrata* biofilms. *Lett Appl Microbiol*. 2012. Vol. 54:383-391.
12. Metwalli KH, Khan SA, Krom BP, Jabra-Rizk MA. *Streptococcus mutans*, *Candida albicans*, and the human mouth: a sticky situation. *PloS Pathog*. 2013. Vol. 9:e1003616.
13. Lemos JA, Quivey RG Jr, Koo H, Abranch es J. *Streptococcus mutans*: a new Gram-positive paradigm? *Microbiology*. 2013. Vol.159:436-445.
14. Falsetta ML, Klein MI, Lemos JA, Silva BB, Agidi S, Sott-Anne KK, Koo H. Novel antibiofilm chemotherapy targets exopolysaccharide synthesis ad stress tolerance in *Streptococcus mutans* to modulate virulence expression in vivo. *Antimicrob Agents Chemother*. 2012. Vol. 56:6201-6211.
15. Rouabhia M, Chmielewski W. Diseases Associated with Oral Polymicrobial Biofilms. *Open Mycol J*. 2012. Vol. 6:27-32.
16. Barbieri DdS'AV, Vicente VA, Fraiz FC, Lavoranti OJ, Svidzinski TIE, Pinheiro RL. Analysis of the in vitro adherence of *Streptococcus mutans* and *Candida albicans*. *Braz J Microbiol*. 2007. Vol.38:624-663.

17. Jarosz LM, Deng DM, van der Mei HC, Crielaard W, Krom BP Streptococcus mutans competence-stimulating peptide inhibits Candida albicans hypha formation. *Eukaryotic Cell*. 2009. Vol. 8:1658-1664.
18. Brogden KM, Guthmiller JM, editors (2008) *Polymicrobial diseases*. Washington: ASM Press.
19. Monteiro DR, Gorup LF, Silva S, Negri M, de Camargo ER, Oliveira R, Barbosa DB, Henriques M. Silver colloidal nanoparticles: antifungal effect against adhered cells and biofilms of *Candida albicans* and *Candida glabrata*. *Biofouling*, 2011. Vol. 27:711-719.
20. Lynch RJ, ten Cate JM. Effect of calcium glycerophosphate on demineralization in an in vitro biofilm model. *Caries Res*. 2006. Vol. 40:142-147.
21. Bowen WH. The cariostatic effect of calcium glycerophosphate in monkeys. *Caries Res*. 1972. Vol. 6:43-51.
22. Grenby TH. Trials of 3 organic phosphorus-containing compounds as protective agents against dental caries in rats. *J Dent Res* 1973 Vol.52:454-461.
23. Duke SA, Rees DA, Forward GC. Increased plaque calcium and phosphorus concentrations after using a calcium carbonate toothpaste containing calcium glycerophosphate and sodium monofluorophosphate. *Caries Res* 1979. Vol. 13:57-59.
24. Nordbö H, Rölla G. Desorption of salivary proteins from hydroxyapatite by phytic acid and glycerophosphate and the plaque-inhibiting effect of the two compounds in vivo. *J Dent Res* 1972. Vol. 51:800-811.
25. Grenby TH, Bull J M. Use of high-performance liquid chromatography techniques to study the protection of hydroxylapatite by fluoride and glycerophosphate against demineralization in vitro. *Caries Res* 1980. Vol. 14:221-232.
26. Naylor MN, Glass RL. A three-year clinical trial of a calcium carbonate dentifrice containing calcium glycerophosphate and sodium monofluorophosphate. *Caries Res* 1979. Vol. 13:39-46.
27. Mainwaring PJ, Naylor MN. A four-year clinical study to determine the caries-inhibiting effect of calcium glycerophosphate and sodium fluoride in calcium carbonate base dentifrices containing sodium monofluorophosphate. *Caries Res* 1983. Vol. 17:267-276.
28. do Amaral JG , Sasaki KT, Martinhon CC, Delbem AC. Effect of low-fluoride dentifrices supplemented with calcium glycerophosphate on enamel demineralization in situ. *Am J Dent*. 2013. Vol 26:75-80.
29. Zaze AC, Dias AP, Amaral JG , Miyasaki ML , Sasaki KT , Delbem AC. In situ evaluation of low-fluoride toothpastes associated to calcium glycerophosphate on enamel remineralization. *J Dent*. 2014. Vol.42:1621-1625.
30. Miranda M, Fernández A, Lopez-Esteban S, Malpartida F, Moya JS, Torrecillas R. Ceramic/metal biocidal nanocomposites for bone-related applications. *J Mater Sci Mater Med*. 2012. Vol. 23:1655-1662.
31. Liu Y, Zhou R, Wu H. Study on the antibacterial activity of four kinds of nano-hydroxyapatite composites against *Enterococcus faecalis*. *Hua Xi Kou Qiang Xue Yi Za Zhi* 2015. Vol. 33:301-305.
32. Furuzono T, Motaharul M, Kogai Y, Azuma Y, Sawa Y. Synthesis and antibacterial evaluation of calcinated Ag-doped nano-hydroxyapatite with dispersibility. *Int J artif órgãos*. 2015. Vol. 38:251-258.
33. Turkevich J, Stevenson PC, Hillier J. A study of the nucleation and growth processes in the synthesis of colloidal gold. *Discuss. Faraday Soc*. 1951. Vol. 11: 55-75.
34. Gorup LF, Longo E, Leite ER, Camargo ER. Moderating effect of ammonia on particle growth and stability of quasi-monodisperse silver nanoparticles synthesized by the Turkevich method. *J Colloid Interface Sci*. 2011. Vol. 15:355-358.

35. Gosh SK, & Pal T. "Interparticle coupling effect on the surface plasmon resonance of gold nanoparticles: from theory to applications". *Chem. Rev.* 2007. Vol. 107:4797.
36. Inoue M, In Y, & Ishida T. "Calcium binding to phospholipid: structural study of calcium glycerophosphate". *Journal of Lipid Research*, 1992. Vol. 33:985.
37. Solomon S, Bahadory M, Jeyarajasingan A, Rutkowsky S, Boritz C. Synthesis and study of silver nanoparticles. *EUA. Journal of Chemical Education*. Vol. 84 February 2007. Vol. 2:322.
38. Morones JR, Elechiguerra JL, Camacho A, Holt K, Kouri JB, Ramírez JT, Yacaman MJ. The bactericidal effect of silver nanoparticles. *Nanotechnology*. 2005. Vol. 16:2346-2353.
39. Pal S, Tak YK, Song JM. Does the antibacterial activity of silver nanoparticles depend on the shape of the nanoparticle? A study of the Gram-negative bacterium *Escherichia coli*. *Appl Environ Microbiol.* 2007. Vol. 73:1712-1720.
40. Bradford A, Handy RD, Readman JW, Atfield A, Mühling M. Impact of silver nanoparticle contamination on the genetic diversity of natural bacterial assemblages in estuarine sediments. *Environ Sci Technol.* 2009. Vol. 15:4530-4536.
41. Durán N, Durán M, de Jesus MB, Seaabra AB, Fávaro WJ, Nakazato G. Silver Nanoparticles: A New View on Mechanistic Aspects on Antimicrobial Activity. *Nanomedicine*. 2015. Vol. 24. pii: S1549-9634(15)00600-0.
42. Feng QL, Wu J, Chen GQ, Cui FZ, Kim TN, Kim JO. A mechanistic study of the antibacterial effect of silver ions on *Escherichia coli* and *Staphylococcus aureus*. *J Biomed Mater Res.* 2000. Vol. 52:662-668.
43. Stoimenov PK, Klinger RL, Marchin GL, Klabunde KJ. Metal Oxide Nanoparticles as Bactericidal Agents. *Langmuir*. 2002. Vol. 18:6679-6686.
44. Busscher HJ, Bos R, van der Mei HC, Handley PS. In *Physical Chemistry of Biological Interfaces*; Baszkin, A., Norde, W., Eds. Marcel Dekker: New York, 2000.
45. Hamouda T, Baker JR Jr. Antimicrobial mechanism of action of surfactant lipid preparations in enteric Gram-negative bacilli. *J Appl Microbiol.* 2000. Vol. 89:397-403.
46. Lynch RJ. Calcium glycerophosphate and caries: a review of the literature. *Int Dent J.* 2004. Vol. 54:310-314.
47. Löffler J, Einsele H, Hebart H, Schumacher U, Hraštnik C, Daum G. Phospholipid and sterol analysis of plasma membranes of azole-resistant *Candida albicans* strains. *FEMS Microbiol Lett.* 2000. Vol. 185:59-63.
48. Lara HH, Romero-Urbina DG, Pierce C, Lopez-Ribot JL, Arellano-Liménez MJ, Jose-Yacaman M. Effect of silver nanoparticles on *Candida albicans* biofilms: an ultrastructural study. *J Nanobiotechnology*. 2015. Vol. 13:91.
49. Vazquez-Muñoz R, Avalos-Borja M, Castro-Longoria E. Ultrastructural analysis of *Candida albicans* when exposed to silver nanoparticles. *PLoS One*. 2014; 9:e108876.
50. Hwang I, Lee J, Hwang JH, Kim K-J, Lee DG. Silver nanoparticles induce apoptotic cell death in *Candida albicans* through the increase of hydroxyl radicals. *FEBS J.* 2012. Vol. 279:1327-38.

Tables and Figures:

Table 1. Minimum inhibitory concentrations (MIC) of %Ag/CaGP nanocomposites against microorganisms tested and silver ions concentrations.

GROUP	Reducing agent	Ag % / GPCa particles	Solvent	MIC ($\mu\text{g/mL}$)		$\mu\text{g Ag}^+/\text{mL}$
				<i>C. albicans</i>	<i>S. mutans</i>	
B1	NaBH ₄	1 / micro*	Isopropanol	>1600	>1600	2.83
B2	NaBH ₄	1 / nano	Isopropanol	400-1600	>1600	4.46
B3	NaBH ₄	10 / micro*	Isopropanol	400-800	>1600	10.81
B4	NaBH ₄	10 / nano	Isopropanol	100-200	>1600	63.34
B5	NaBH ₄	1 / micro*	Water	>1600	>1600	0.44
B6	NaBH ₄	1 / nano	Water	>1600-	>1600	2.76
B7	NaBH ₄	10 / micro*	Water	>1600	>1600	5.97
B8	NaBH ₄	10 / nano	Water	>1600-	>1600	15.63
C1	Na ₃ C ₆ H ₅ O ₇	1 / micro*	Water	156.2-312.5	1250	305.43
C2	Na ₃ C ₆ H ₅ O ₇	1 / nano	Water	156.2-312.5	1250	168.14
C3	Na ₃ C ₆ H ₅ O ₇	10 / micro*	Water	39.05	312.5-625	506.73
C4	Na ₃ C ₆ H ₅ O ₇	10 / nano	Water	19.5-39.05	156.2-312.5	487.95

*Commercial form (80% β -isomer and 20% rac- α -isomer, G6626, Sigma Chemical Co, St Louis, Missouri, USA)

Table 2. Minimum inhibitory concentrations (MIC) and silver ions concentration of control solutions.

Controls	MIC ($\mu\text{g/mL}$)		$\mu\text{g Ag}^+/\text{mL}$
	<i>C. albicans</i>	<i>S. mutans</i>	
Na ₃ C ₆ H ₅ O ₇ /NH-PM	>400	>400	-
NaBH ₄ / NH-PM	>1500	>1500	-
nanoAg (Na ₃ C ₆ H ₅ O ₇)	7.8	250	107.25
nanoAg (NaBH ₄)	62.5	125	576.19
AgNO ₃	5.31	21.25	-
β -GPCa nano	>5000	>5000	-
β -GPCa comercial	>5000	>5000	-

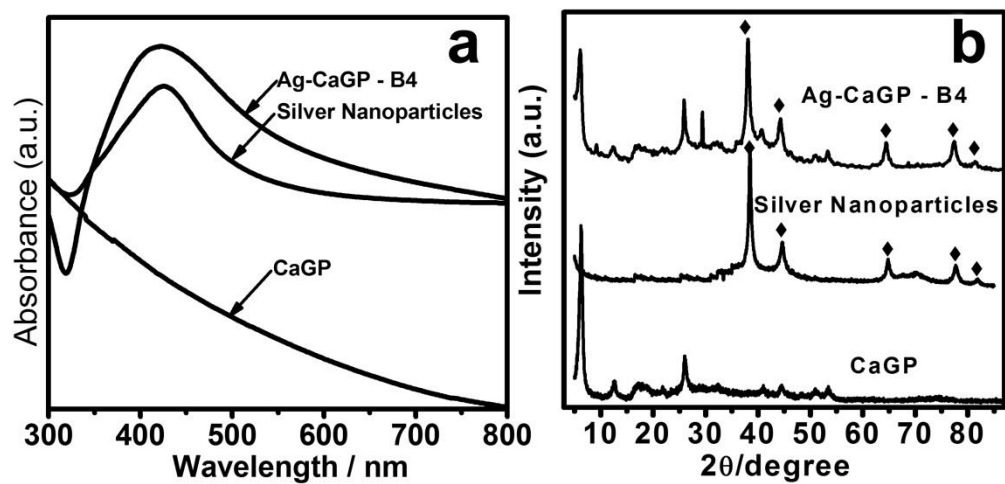


Figure 1. a) UV–Visible spectrum and b) XRD pattern of Ag-CaGP (B4 group) nanocomposite, silver nanoparticles and CaGP.

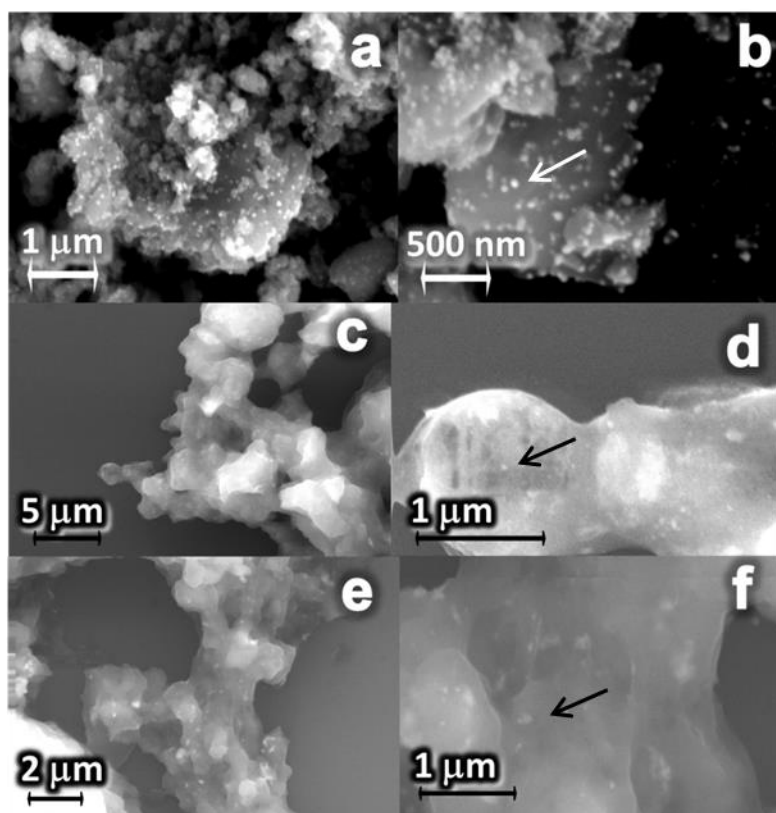


Figure 2. SEM images of the Ag-CaGP nanocomposites: B4 (a and b), C4 (c and d) and B8 (e and f) in different magnifications. The arrows indicate silver nanoparticles on the surface of CaGP in B4 and in the bulk of CaGP in C4 and B8.

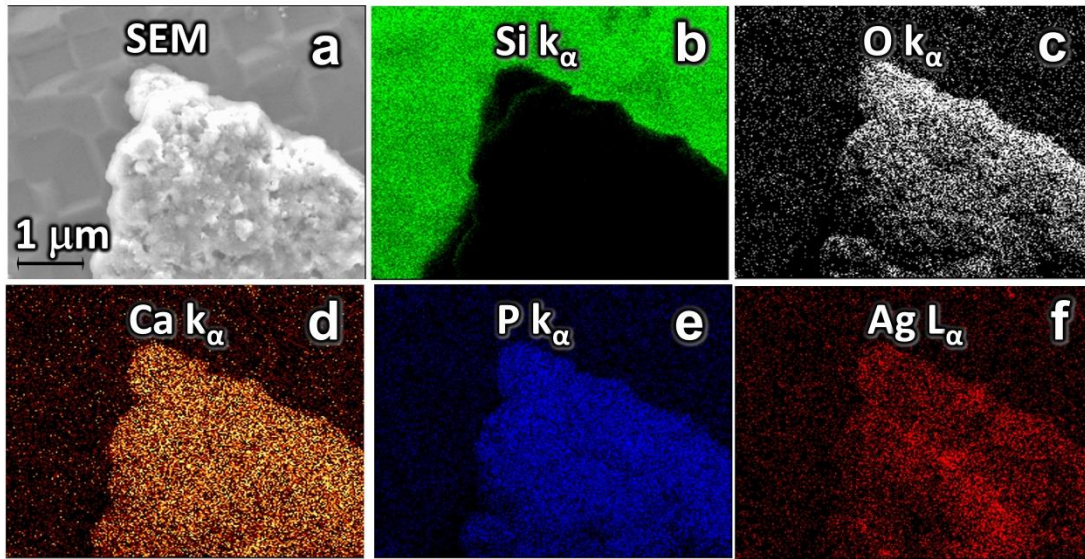


Figure 3. SEM and EDS mapping of the 2D elements issuance Si $K\alpha$, O $K\alpha$, P $K\alpha$, Ca $K\alpha$ and Ag $K\alpha$ false color. Analysis of the distribution of silver nanoparticles on the Ag-CaGP for sample B4: a) SEM image; b) chemical mapping of silicon element present in the substrate, where the electron beam was focused directly on the substrate and is showed in green color, and the dark regions the beam was focused in Ag-CaGP nanocomposite B4; c-f) oxygen, calcium, phosphorus and silver, respectively, demonstrating they are constituents of the Ag-CaGP.

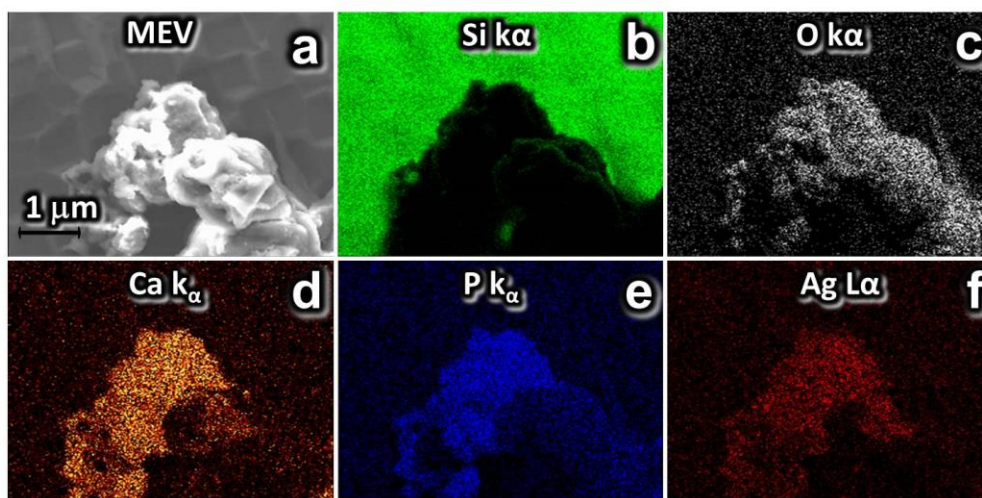


Figure 4. SEM and EDS mapping of the 2D elements issuance Si K α , O K α , P K α , Ca K α and Ag K α false color. Analysis of the distribution of silver nanoparticles on the Ag-CaGP for sample C4: a) SEM image; b) chemical mapping of silicon element present in the substrate, where the electron beam was focused directly on the substrate and is showed in green color, and the dark regions the beam was focused in Ag-CaGP nanocomposite C4; c-f) oxygen, calcium, phosphorus and silver, respectively, demonstrating they are constituents of the Ag-CaGP.

CAPÍTULO 2

Synthesis of silver nanoparticles and calcium glycerophosphate using peel extract of pomegranate: a green route to produce a nanocomposite to control important oral pathogens

Synthesis of silver nanoparticles and calcium glycerophosphate using peel extract of pomegranate: a green route to produce a nanocomposite to control important oral pathogens

Abstract

The aim of this study was to synthesize and characterize a biomaterial containing silver nanoparticles (Ag) and calcium glycerophosphate (CaGP) (Ag/CaGP) by green route using peel extract of pomegranate as reductor agent. Its antimicrobial action was evaluated by broth microdilution method (MIC) in accordance with the Clinical Laboratory Standards Institute, against reference strains of *Candida albicans* (ATCC 10231) and *Streptococcus mutans* (ATCC 25175). The peel extracts were obtained by percolation (ethanol 70%) in which the ellagic acid was quantified by high performance liquid chromatography and the total phenols were determined by colorimetric method using Folin-Denis reagent and gallic acid as standard. For the synthesis of Ag/CaGP in a solution of deionized water heated to 90 ° C 0.25 g of CaGP were added, followed by 0.042 g of silver nitrate (AgNO₃), 0.5 mL of ammonium salt of polymethacrylic acid (NH-PM), and then 0.07 g of peel extract of pomegranate, totalizing a final volume of 10 mL. AgNP was prepared in the same conditions and with no addition of CaGP. Ag/CaGP was characterized by UV-Vis Spectroscopy, XRD (X-ray diffraction spectroscopy), and absorption spectroscopy by scanning electron microscopy (SEM) and mapping in 2D by EDX (electron dispersive X-ray). MIC was assessed visually after 48 hours of incubation at 37° C for *C. albicans* and after 24 hours under microaerophilic condition for *S mutans*. The ellagic acid of total phenols values were, respectively, 4.21 mg/g and 158.61 mg/g. The analytical techniques and SEM images indicated the formation of AgNP in association or not with CaGP. Also, both Ag/CaGP and AgNP were effective against tested microorganisms, being the MIC values for *C. albicans* 156.3 µg/mL of Ag/CaGP and 312.5 µg/mL of AgNP, and for *S. mutans* 156.3 µg/ml of Ag/CaGP and 78.1 µg/ml of AgNP. Therefore, the green route using pomegrate peel extract promoted the formation AgNP in association with CaGP, and the biomaterial produced was effective

against important oral pathogens as *C. albicans* and *S. mutans* which stimulate its use in dental compounds to fight against dental caries.

Keywords: Nanoparticles, Punicaceae, *Candida albicans*, *Streptococcus mutans*

Introduction

Nanotechnology appeared as a new science that involves the creation of materials engineered at nanoscale [1], and as an alternative tool for developing technologies with new properties to attend the increasing demand of different areas of life and industrial sectors for advanced functional materials [2]. The application of this new technology has been expressively used in biodiagnostics [3], catalysis [4,5], textiles applications [6], biotechnology [7], biosensors [8], bioelectronics [9], water filtration system [10], as well as in biomedical field [4,11].

The use of nanotechnology for synthesizing silver nanoparticles (AgNP) is very common and it has been explored due to its numerous applications including antiviral [12-14], antibacterial [12;14], , antifungal [12;14], anti-inflammatory [12;14] and anti-carcinogenic potential [13].

According to some authors, the antimicrobial activity of silver nanoparticles (AgNP) would be related with the release of Ag^+ , leading to toxicity and bacterial death [15]. Silver ions would bind to electron donor groups in biological molecules containing sulfur or nitrogen, resulting in defects in the bacteria cell membrane and causing the loose of the cell contents and the bacterial death [16,17]. In addition, AgNPs would generate reactive oxygen species (ROS) [18,19], including hydroxyl radicals [20,21], superoxide [20-22], hydrogen and peroxide [21] and cause oxidative stress that might trigger inflammatory response [23]. When used in a non-cytotoxic dose it would induce chromosomal abnormality, DNA damage and a possible mutagenicity preventing the cell reproduction [24].

However, although several characteristics make AgNPs interesting as a therapeutic proposal it have also been identified as toxic for human health inducing undesired effects [25]. However, its potential cytotoxic depends of several factors such as exposure time, dose, shape, size, surface chemistry, presence of stabilizing agents and mammalian cell types [26].

Thus, an alternative to try reducing the cytotoxicity of AgNP is use natural products replacing the harmful chemicals in reduction of Ag^+ ions. Various products such as plant extracts and phytochemicals are employed in this sustainable initiative [27].

Recent studies showed the involvement of phenolic compounds present in plants, such as the responsible for the ion reduction, excluding the use of chemical ingredients [28]. The literature indicates the *Punica granatum* has over 124 phytochemicals compounds [29] including polyphenols, that exhibit favorable properties against various inflammatory and antioxidants disorders [29,30]. Studies presented that among all compounds, the ellagitannins (ellagic acid, punicalagin, punicalin and gallagic acid) are the most active antioxidants contained in the peel extract, and synergistic activity between these compounds potentiating its antioxidant effects [30,31]. It is believed that polyphenols including ellagic acid and gallic acid are responsible for the reduction of Ag^+ ions and the stabilization of AgNP [32,33].

The association of AgNP with hydroxyapatite (HA), which is present in bone and teeth, has been investigated for its many beneficial properties [34] in the medical and dental field. Coating of orthopedic prostheses and dental implants to improve the process of osseointegration has been strongly explored in the literature [35-37]. Moreover, nanomaterials containing calcium phosphates for the treatment of lesions of dental caries have also been investigated by several authors [38-42]. Calcium glycerophosphate (CaGP) is an organic phosphate salt with anti-caries properties early demonstrated in in vivo assays with monkeys [43] and rats [44,45]. Although the mechanism of action of this phosphate still not well understood, it is believed in their direct interaction with the enamel inorganic salts [46], besides promotes a buffering effect [43] and raise the calcium and phosphate levels into the dental biofilm [47].

So considering the biosynthesis a simple process with formation of highly stable AgNP at room temperature [28,48] and taking advantages of CaGP remineralization properties, the development of a new nanobiomaterial with both antimicrobial and anti-caries properties allowed

relevant benefits to control the caries which is the most common dental disease in development countries [49]. Thinking on this way and following the principle of green synthesis by using *Punica granatum* extracts, the aiming of the present study was to synthesize AgNP and Ag-CaGP using extract of pomegranate peel characterizing them by UV-Vis, X-Ray Diffraction, SEM and EDX, as well as evaluating their antimicrobial effect against two common oral pathogens.

Material and Method

Pomegranate peel extract

Chemicals, solvents and materials

Ellagic acid (EA) was acquired from Fluka(Germany - 95.0%, batch BCBN4398V) and gallic acid (GA) from Sigma-Aldrich (Sigma-Aldrich Chemical Co, St Louis, USA, 97.5%, batch 071M0031V). Some chemical standards were purchased from Phytolab (Bayern - Mittelfranken, Germany) as punicalagin (PG) (batch 17811260), punicalin (PN) (batch 17911287) and corilagin (CG) (batch 17911252), and their purity was all > 98%. Folin-Denis reagent was prepared using phosphomolybdic-phosphotungstic reagent (Qhemis - High Purity, Hexis, São Paulo, Brazil), batch 13081090, Vetec, Rio de Janeiro, Brazil , batch DCBD0807V) and sodium carbonate (Cinética, São Paulo, Brazil - 99.5%, batch 22317). The high performance liquid chromatography (HPLC) grade methanol was supplied by J.T. Baker (Mexico city, Mexico), and purified water was obtained using a Milli-Q Direct Q-5 filter system (Millipore, Bedford, USA). Analytical reagents acetic acid, sodium hydroxide, hydrochloric acid were purchased from Synth (Labsynth, Diadema, Brazil).

Plant material

This study was performed on peels of pomegranate fruit which was bought from a local supermarket in São Paulo (CEAGESP - Company Warehouses and General Warehouses of São Paulo). The fruits were cultivated in the northeastern part of the State of São Paulo and harvested in May of 2015. A specimen of the plant drug was deposited in the Herbarium of the University of São Paulo, Ribeirão Preto, SP, Brazil. Pomegranates were washed with water and manually peeled. The peels were dried in an incubator at 50°C, and grounded into powder form using a blender [50]. The powder was then filtered through a 42-mesh sieve to obtain standardized particle size [51].

Preparation of the peel extract

The powder of the peels was submitted to an extraction with ethanol at 70%v/v by maceration and percolation process [52]. 30 g of peels powder were added into an Erlenmeyer containing 100 mL of an ethanol solution (70%v/v) and waited to stand to approximately 1 hour. Following, the solution was poured out in a percolator and the peel extract was concentrated in a rotary evaporator under reduced pressure and controlled temperature (40-60°C) [51]. After the solvent evaporation, the soft extract was resolubilized in deionized water to be followed used as the reducer agent to synthesize AgNP and Ag-CaGP compounds.

Total phenolic content

Total phenols (TP) contents in the extract were determined by colorimetric method [53] using Folin-Denis reagent and gallic acid as standard. It was calculated as gallic acid equivalents (GAE) per gram. The extracts (70-95mg) were firstly diluted in water (50ml), and were properly homogenated using a vortex and, then, remained for 30 minutes in UV-bath. 0.5 mL of the sample was transferred to a new flask containing 2.5 mL of reagent of Folin-Denis and 5.0 mL of 29% sodium carbonate. The samples were kept at room temperature (25°C) for 30 minutes. Total phenols of the extract as gallic acid equivalents were obtained using the absorbance of the extract measured at 760 nm as input to the standard equation.

Ellagic acid content

To determine the ellagic acid content (EAC), the extracts previously diluted in methanol were properly homogenated using a vortex and then remained for 30 minutes in UV-bath, were filtered and subjected to HPLC analysis (Shimadzu apparatus equipped with a CBM controller, LC-20AT quaternary pump, a SPD-M 20A diode-array detector and auto sampler, Shimadzu LC solution software, version 1.21 SP1) using a 100 mm x 2.6 mm Shim pack ODS C18 column.

The mobile phase used for ellagic acid was methanol and acetic acid aqueous solution 2% using a elution gradient (0-7min, 20-72.5% v/v methanol, 7-7.5 min, 72.5-95% v/v methanol, 7.5-8.5 min. 95% v/v methanol, 8.5-9 min 95-20% v/v methanol, 9-10 min 20% v/v methanol) with a flow rate of 1.0 mL min^{-1} , and oven temperature of 25°C . The eluted samples were detected by UV detector at 254 nm. Calibration curve was constructed by plotting the peak area (y) against concentration in $\mu\text{g mL}^{-1}$ of standard solutions (x). The standard equation obtained from the curve was used for quantification of ellagic acid as mg/g extract of sample.

All assays were carried out in triplicates and the ellagic acid quantification was reported.

Synthesis and characterization of AgNP and Ag-CaGP

CaGP were nanoparticulated at the Interdisciplinary Laboratory of Electrochemistry and Ceramics (Department of Chemistry, Federal University of São Carlos, São Carlos, SP, Brazil). To prepare the CaGP nano-sized, 70 g of pure (commercial) β -calcium glycerophosphate (80% β -isomer and 20% rac- α -isomer, CAS 58409-70-4, Sigma-Aldrich) were ball milled using 500 g of zirconia spheres (diameter of 2 mm) in 1 L of isopropanol (Merck KGaA, Darmstadt, Deutschland, Germany). After 24 h, the powders were separated from the alcoholic media and ground in a mortar. To characterization of the nanoparticles of CaGP, transmission electronic microscopy (FEG-VP Supra 35 electron microscope; Carl Zeiss, Jena, Germany) was realized confirming the medium size of 10 nm with a regular distribution and without alteration of the crystalline structure.

AgNP and Ag/CaGP were synthesized by means of the Turkevich et al. [54] and Gorup et al. [55] methods with some modifications. For the synthesis of Ag/CaGP in a solution of deionized water heated to 90°C were added 0.25 g of CaGP, 0.042g of silver nitrate (AgNO_3 , Merck KGaA), 0.5mL of ammonium salt of polymethacrylic acid (NH-PM, Polysciences Inc., Warrington, Pennsylvania, USA), and then 0.07 g of peel extract of pomegranate totalizing a final volume of 10 mL. AgNP sample was prepared in the same conditions with no addition of CaGP.

The formation of AgNP and Ag/CaGP was confirmed by UV-Visible spectroscopy (spectrophotometer Shimadzu MultiSpec-1501, Shimadzu Corporation, Tokyo, Japan) and X-ray diffraction (XRD) (Diffractometer Rigaku DMax-2000PC, Rigaku Corporation, Tokyo, Japan). The particles morphology was also characterized by scanning electron microscopy (SEM) on a Zeiss Supra 35VP microscope (S-360 microscope, Leo, Cambridge, Massachusetts, USA) with field emission gun electron effect (FEG-SEM) operating at 10 kV. It was also performed analyzes by Energy Dispersive X-Ray Detector, EDX) with mapping in 2D. 2D images were constructed by analyzing energy released from the emission Si K α , O K α , P K α , Ag L α 1 e Ca K α . At the images, it is attributed false color to highlight the silver and for oxygen, silicon, phosphate and calcium.

Antimicrobial activity of AgNP and Ag-CaGP

The minimum inhibitory concentration (MIC) of each compound was performed using the microdilution method According to the Clinical Laboratory Standards Institute (CLSI: M27-A2; M07-A9) guidelines with some modifications. *Candida albicans* and *Streptococcus mutans* were obtained from American Type Culture Collection (ATCC 1031 and ATCC 25175), and subcultured respectively on Sabouraud Dextrose Agar (SDA, Difco) aerobically and Miler Hinton (MH, Difco, Le Pont de Claix, France) at 5% of CO₂, both for 24 h at 35°C. Microorganisms were adjusted in saline 0.85% to a turbidity equivalent to 0.5 McFarland Standard (1 x 10⁶ *C. albicans* CFU/mL and 1 x 10⁸ *S. mutans* UFC/mL). Following, *C. albicans* inoculum was diluted 100-fold (1 x 10⁴ CFU/mL) in Roswell Park Memorial Institute medium (RPMI-1640, Sigma-Aldrich), and *S. mutans* 20-fold in Miller Hinton (Difco, France) supplemented with 5% of glucose to a final cell concentration of 5 x 10⁶ CFU/mL.

A volume of 100 μ l of each solution to be tested (Table 1) was added into the well containing 100 μ l of a specific medium, and sequentially the serially dilution was carried out ranging from 1:2 to 1:512. After the dilutions were done, 5 μ L of *C. albicans* and 10 μ L of *S. mutans* suspension were

added to each well and the plates were incubated aerobically for 48 h for *C. albicans* and in 5% CO₂ for 24 h for *S. mutans* both at 35°C.

All MIC determinations were carried out in triplicate in three different occasions.

Results and discussion

Pomegranate peel extract: total phenolic content and ellagic acid content

Pomegranate peel extracts has been reported to present antioxidant, anti-inflammatory and antimicrobial activities [56,57]. It is a rich source of alkaloids and polyphenols [58], and one of the main components responsible for its potential health benefits is ellagic acid [28]. Besides tannins such as punicalagin, punicalin and corilagin might be related to the antimicrobial action of this fruit. [59].

The ethanol extraction by maceration and percolation method was selected since allow the extraction products from high quantities of peel powder until its total depletion. In the present study, the total phenolic contents in the soft extract (expressed in gallic acid) and the ellagic acid were respectively 158.61 mg/g and 4.21 mg/g. Several factors interfere on the quantification of polyphenols, including the cultivation conditions such as soil, water and sunlight [60], as well as the selection of solvent is relevant to extract the bioactives products with acceptable yields and strong antioxidant and antimicrobial activity [61].

It is also important to consider that correct identification and quantification of polyphenols, mainly consisting of ellagitannins [62], is difficult due to their structural complexity and diversity, as well as the lack of commercially available standards [63]. Moreover, the diversity of extraction methods would not enable the comparison the total phenols and ellagic acid quantifications presented in this study with mostly works in the literature.

Synthesis and characterization of AgNP and Ag/CaGP

In this study, biosynthesis processes using peels of pomegranate as a reducing agent to obtain AgNP and the subsequent addition of these nanoparticles with CaGP was carried out and characterized.

Deionized water was used a solvent for the AgNP and Ag/CaGP synthesis. It was heated to 90°C to advance the process of silver ion reduction [64]. Silver nitrate was then added, followed for the surfactant agent (NH-PM) [65], and finally the pomegranate peel extract previously diluted in water (7 mg/mL) to promote the formation of AgNP. Whereas for the synthesis of Ag/CaGP the first compound added to hot water was CaGP.

In both syntheses, there was an immediate change in color, becoming dark brown, characteristic of the formation of AgNP [28,64,66]. After a very few hours of synthesis, the compound formed is deposited on the glass bottom and formed a supernatant liquid with light color [28].

Pomegranate peel extract antioxidant activity might be responsible for the reduction of metal ions [28]. Ahamad et al. [28] explained the reduction capacity of the plant is mostly due to their redox properties, which would act in absorbing and neutralizing free radicals, quenching singlet and triplet oxygen, or decomposing peroxides. The antioxidant action of punicalagin also would promote the formation of H⁺ radicals which in turn reduces the size of silver particles to nanosize [28]. So, the significant potential reduction of the pomegranate peel extract was an important factor to choose this plant for the biosynthesis of AgNP [28].

UV-Vis and XRD analysis

The reduction of silver ions by pomegranate peel extract and formation of AgNP was confirmed by the presence of a plasmon band between 420 and 450 nm (UV-Vis), and was observed in both compounds synthesized by green route (AgNP and Ag/CaGP) (Figure 1a). It indicated that the addition of CaGP did not interfere on the formation of AgNP. The major constituents of pomegranate peel extracts are polyphenols mainly ellagitannins, such as ellagic acid and gallic acid [63,66]. They are soluble in water and are involved in inter and intra bonding of molecular hydrogen [66]. It might be these constituents act in the silver nanoparticles formation.

The results in this study are consistent with studies in the literature where the peel extract of pomegranate was used for the synthesis of AgNP [28]. In addition, other parts of this fruit as pulp juice have shown also the ability to reduce silver ions from AgNO₃ [67,68]. Thus, our work confirmed that the compounds present in the pomegranate peel extract were able to reduce and stabilize the AgNP and, interestingly, the addition of CaGP did not interfere in this process.

The typical XRD pattern of the prepared nanopowder of CaGP showed diffraction peaks at $2\theta = 6.30^\circ, 12.3^\circ, 26.4^\circ, 41.1^\circ, \text{ and } 44.2^\circ$ (Figure 1b) and the corresponding crystallographic form (PDF № 1-17) [69]. The typical XRD pattern of the silver nanoparticles (Figure 1b) showed diffraction peaks at $2\theta = 38.2^\circ, 44.4^\circ, 64.6^\circ, 77.5^\circ, \text{ and } 81.7^\circ$, which can be indexed to (111), (200), (220), (311), and (222) planes of pure silver with face-centered cubic system (PDF № 04-0783).

SEM and Mapping in 2D for EDX analyzes

It is observed in the SEM images the presence of AgNP obtained by the pomegranate peel extract (Figure 2). This AgNP exhibited a relatively uniform dispersion and spherical shape with size of approximately 50 nm (Figure 2b). This data strengthens that the compounds present in the peel extract of pomegranate have ability to reduce and stabilize these AgNP in an aqueous medium [28]. For the Ag/CaGP, the formation of clusters is noted with silver nanoparticles into the CaGP bulk (Figure 3). As hydroxyapatite [70,71], CaGP is not well solubilized in aqueous media. It might lead the agglomeration of these particles, and the silver nanoparticles associated with them during the synthesis reaction were enclosed in the CaGP mass.

Figure 4 shows the EDX images mapped in 2D and set up by the analyzing the energy released from the issuance Si K α , O K α , P K α , Ca K α and Ag K α , indicating the distribution of these elements on the demarcated area in the micrograph.

Antimicrobial activity of AgNP and Ag-CaGP

Both AgNP and Ag/CaGP presented antimicrobial effect against ATCC strains of *C. albicans* and *S. mutans*. The best MIC values of AgNP and Ag/CaGP for *C. albicans* were at 312.5 µg/ml and 156.3 µg/ml of total silver content in each compound. While for *S. mutans* these values were 78.1 µg/ml for AgNP and 156.3 µg/ml for Ag/CaGP (Table 1).

The exact mechanism of antimicrobial action of AgNP against *C. albicans* has been elucidated for some authors [72,73]. Through TEM images, Lara et al. [72] demonstrated an interaction of these particles with *C. albicans* cell wall leading to a disruption of their external part and then yielding permeabilization in the inner parts of the cell wall and the cell membrane which allowed AgNP to get into the yeast. Although the chemical arrangement of external membrane of *S. mutans* differs greatly from that of *C. albicans*, they are mainly structured by phospholipids which are charged negatively due to the groups of phosphate [72,74] incorporated in the hydrophilic head [72,75] which could be targeted by membrane disturbing cationic AgNP [72].

Moreover, the release of silver ions from AgNP has also been cited for some authors [76-78], and the electrostatic attraction between the negative charges present on the membrane of microorganisms and the positive charge that of the silver nanoparticles [79] would be the major pathway relevant in the antibacterial activity involving Ag⁺ ions [80].

Although AgNPs had shown antimicrobial activity against both microorganisms, the effective concentration of silver were higher for *C. albicans* than for *S. mutans*. One of the reasons that could explain that difference, would be the another mechanism of action of AgNP. Once inducing permeability of the membranes and penetrating into the microorganism cell these particles would react with some proteins by combining with thiol groups inactivating some enzymatic activity and leading in a DNA condensation. It would avoid its replicating ability [81,82], and be happen more easily in prokaryotes organisms than eukaryotes ones. Interestingly, for *C. albicans*, when CaGP was added to AgNP its effectiveness was almost 2-fold higher than AgNP alone. This may be due to the

buffer effect caused by CaGP [83], once *C. albicans* have the ability to produce and tolerate acidic environments [72] namely a source of calcium and phosphate may raise the pH [41,42] and influence growth of this yeast.

Amaral et al. [41] and Zaze et al. [42] assessed the positive influence of the CaGP in dental demineralization and remineralization process. They proposed several mechanisms of action including direct interaction with enamel, where CaGP would reduce acid-dissolution by buffering the pH of dental biofilm, reducing their mass and modifying the biofilm metabolism, as well as would elevate the calcium and/or phosphorus levels in dental biofilm [83,84]. Reinforcing that, this phosphate presents properties that can act positively against microorganisms. However, in the case of *S. mutans* our results directed to the opposite side, where the silver effective concentration needed to be higher when AgNP was associated to CaGP. Probably there would be potential sites on the AgNP surface which may have interacted with *S. mutans* membrane and could have been lost when CaGP was added to. Further studies including ultrastructure micrograph analysis of the microorganism membranes could elucidate the possible interaction between green nanocomposites with silver and microorganisms as well as their mechanisms of action.

In conclusion and considering the possible side effects of AgNP produced by conventional chemical routes to both, workers at manufacturing them and consumers exposed to these particles, these particles and its association with CaGP greenly synthesized is very promising for future development of dental biomaterials due to its efficacy against a Gram positive bacteria (*S. mutans*) and a fungus (*C. albicans*).

Acknowledgements:

This study was supported by: São Paulo Research Foundation (FAPESP, Process 2013/24200-9 and 2014/08648-2), Brazil; and Coordination for the Improvement of Higher Education Personnel (Capes, Process 88887.068358/2014-00 and 88881.030445/2013-01), Brazil.

References:

1. Baer DR, Burrows PE, El- Azab AA. Enhancing coating functionality using nanoscience and nanotechnology. *Progress in Organic Coatings*. 2003. Vol. 47: 342-356.
2. Roco MC, Bainbridge WS. Societal implications of nanoscience and nanotechnology: Maximizing human benefit. *Journal of Nanoparticle Research*. 2005. Vol. 7: 1-13.
3. Dykman L, Khlebtsov N. Gold nanoparticles in biomedical applications: recent advances and perspectives. *Chemical Society Reviews*. 2012. Vol. 41: 2256-2282.
4. Faria AF, Martinez DST, Meira SMM, Moraes ACM, Brandelli A, Filho AGS, Alves OL. Anti-adhesion and antibacterial activity of silver nanoparticlessupported on graphene oxide sheets. *Colloids and Surfaces B: Biointerfaces*. 2014. Vol. 113: 115-124.
5. Zhang Y, Cui X, Shi F, Deng Y. Nano-gold catalysis in fine chemical synthesis. *Chemical Review*. 2012. Vol.112: 2467-2505.
6. El-Nour KMMA, Eftaiha A, Al-Warthan A, Ammar RAA. Synthesis and applications of silver nanoparticles. *Arabian Journal of Chemistry*. 2010. Vol. 3: 135-140.
7. Lin Y, Li J, Wang J, Li Z, Wang Y. Graphene and graphene oxide: biofunctionalization and applications in biotechnology. *Trends in Biotechnology*. 2011. Vol. 29, No. 5: 205-212.
8. Holzinger M, Goff AL, Cosnier S. Nanomaterials for biosensing applications: a review. *Frontiers in Chemistry/Analytical Chemistry*. 2014. Vol 2, Article 63: 1-10.
9. Göpel W. Bioelectronics and nanotechnologies. *Biosensors & Bioelectronics*. 1998. Vol.13:723-728.
10. Qu X, Alvarez PJJ, Li Q. Applications of nanotechnology in water and wastewater treatment. *Water Research*. 2012. Vol 47: 3931-3946.
11. Dash SS, Bag BG. Synthesis of gold nanoparticles using renewable Punica granatum juice and study of its catalytic activity. *Applied Nanoscience*. 2014. Vol. 4: 55-59.
12. Ge L, Li Q, Wang M, Ouyang J, Li X, Xing MM. Nanosilver particles in medical applications: synthesis, performance, and toxicity. *International Journal Nanomedicine*. 2014. Vol. 9:2399-2407.
13. Wei L, Lu J, Xu H, Patel A, Chen ZS, Chen G. Silver nanoparticles: synthesis, properties, and therapeutic applications. *Drug Discov Today*. 2015. Vol 20:595-601.
14. Kim TY, Cha SH, Cho S, Park Y. Tannic acid-mediated green synthesis of antibacterial silver nanoparticles. *Arch. Pharm. Res*. 2016.
15. Yang X, Gondikas AP, Marinakos SM, Auffan M, Liu J, Kim HH. Mechanism of silver nanoparticle toxicity is dependent on dissolved silver and surface coating in *Caenorhabditis elegans*. *Environmental Science & Technology*. 2012. Vol. 46: 1119-1127.
16. Damm C, Münstedt H, Rösch A. The antimicrobial efficacy of polyamide 6/silver-nano- and microcomposites. *Materials Chemistry and Physics*. 2008. Vol. 108: 61-66.
17. Panáček A, Kvítek L, Prucek R. Silver colloid nanoparticles: synthesis, characterization, and their antibacterial activity. *Journal of Physical Chemistry B*, 2006. Vol. 110: 16248-16253.
18. Fu PP, Xia Q, Hwang HM, Ray PC, Yu H. Mechanisms of nanotoxicity: Generation of reactive oxygen species. *Journal of Food and Drug Analysis*. 2014. Vol 22: 64-75.
19. Foldbjerg R, Dang DA, Autrup H. Cytotoxicity and genotoxicity of silver nanoparticles in the human lung cancer cell line, A549. *Inorganic Compounds Archives of Toxicology*. 2011. Vol 85: 743-750.
20. Guo JZ, Cui H, Zhou W, Wang W. Ag nanoparticle-catalyzed chemiluminescent reaction between luminol and hydrogen peroxide. *Journal of Photochemistry and Photobiology A: Chemistry*. 2008. Vol. 193: 89-96.

21. Inoue Y, Hoshino M, Takahashi H, Noguchi T, Murata T, Kanzaki Y, Hamashima H, Sasatsu M. Bactericidal activity of Ag–zeolite mediated by reactive oxygen species under aerated conditions. *Journal of Inorganic Biochemistry*. 2002. Vol 92: 37-42.
22. Park HJ, Kim JY, Kim J, Lee JH, Hahn JS, Gu MB, Yoon J. Silver-ion-mediated reactive oxygen species generation affecting bactericidal activity. *Water Research*. 2009. Vol. 43: 1027-1032.
23. Prasad RY, McGee JK, Killius MG, Suarez DA, Blackman CF, De Marini DM, Simmons SO. Investigating oxidative stress and inflammatory responses elicited by silver nanoparticles using high-throughput reporter genes in HepG2 cells: Effect of size, surface coating, and intracellular uptake. *Toxicology in Vitro*. 2013. Vol. 27: 2013-2021.
24. Zhang T, Wang L, Chen Q, Chen C. Cytotoxic Potential of Silver Nanoparticles. 2014. *Yonsei Medical Journal*. Vol.55: 283-291.
25. Barbosa DB, Monteiro DR, Satie A, Gorup LF, Delbem ACB, Pessan JP, Camargo ER, Agostinho AM et al. 2014. *Encyclopedia of Biomedical Polymers and Polymeric Biomaterials*. Doi: 10.1081 IE-EBPP- 120051066
26. Ray PC, Yu H, Fu PP. Toxicity and Environmental Risks of Nanomaterials: Challenges and Future Needs. *Journal of Environmental Science and Health, Part C Environmental Carcinogenesis and Ecotoxicology Reviews*. 2009. Vol. 27:1-35.
27. Park Y, Hong YN, Weyers A, kim YS, Linhardt RJ. Polysaccharides and phytochemicals: a natural reservoir for the green synthesis of gold and silver nanoparticles. *IET Nanobiotechnology*. 2011. Vol. 5: 69-78.
28. Ahmad N, Sharma S, Rai R. Rapid green synthesis of silver and gold nanoparticles using peels of *Punica granatum*. *Advanced Materials Letters*. 2012. Vol. 3:376-380.
29. Akhtar S, Ismail T, Fraternali D, Sestili P. Pomegranate peel and peel extract: chemistry and food features. *Food Chemical*. 2015. Vol 1:417-425.
30. Heber D. Pomegranate Ellagitannins. *Herbal Medicine: Biomolecular and Clinical Aspects*. 2nd edition. 2011.
31. Henning SM, Zhang Y, Seeram NP, Lee RP, Wang P, Bowerman S, Heber D. Antioxidant capacity and phytochemical content of herbs and spices in dry, fresh and blended herb paste form. *International Journal of Food Sciences and Nutrition*. 2011. Vol. 62: 219-225.
32. Edison TJ, Sethuraman MG. Biogenic robust synthesis of silver nanoparticles using *Punica granatum* peel and its application as a green catalyst for the reduction of an anthropogenic pollutant 4-nitrophenol. *Spectrochim Acta A Mol Biomol Spectrosc*. 2013. Vol. 104:262-2644.
33. Kumari A, Guliani A, Singla R, Yadav R, Yadav SK. Silver nanoparticles synthesised using plant extracts show strong antibacterial activity. *IET Nanobiotechnol*. 2015. Vol. 9: 142-152
34. Jarcho M. Calcium phosphate ceramics as hard tissue prosthetics. *Clin Orthop Relat Res*. 1981. Vol. 157: 259-278
35. Vahabzadeh S, Roy M, Bandyopadhyay A, Bose S. Phase stability and biological property evaluation of plasma sprayed hydroxyapatite coatings for orthopedic and dental applications. *Acta Biomater*. 2015. Vol.17:47-55.
36. Kwon YD, Yang DH, Lee DW. A Titanium Surface-Modified with Nano-Sized Hydroxyapatite and Simvastatin Enhances Bone Formation and Osseointegration. *J Biomed Nanotechnol*. 2015. Vol. 11:1007-1015.
37. Karamian E, Khandan A, Motamedi MR, Mirmohammadi H. Surface characteristics and bioactivity of a novel natural HA/zircon nanocomposite coated on dental implants. *Biomed Res Int*. 2014;2014:410627.

38. Naylor MN, Glass RL. A 3-year clinical trial of calcium carbonate dentifrice containing calcium glycerophosphate and sodium monofluorophosphate. *Caries Res.* 1979. Vol. 13: 39-46.
39. Mainwaring PJ, Naylor MN. A four-year clinical study to determine the caries-inhibiting effect of calcium glycerophosphate and sodium fluoride in calcium carbonate base dentifrices containing sodium monofluorophosphate. *Caries Res.* 1983. Vol. 17:267-276.
40. Lynch RJ, ten Cate JM. Effect of calcium glycerophosphate on demineralization in an in vitro biofilm model. *Caries Res.* 2006. Vol.40:142-147.
41. do Amaral JG, Sasaki KT, Martinhon CC, Delbem AC. Effect of low-fluoride dentifrices supplemented with calcium glycerophosphate on enamel demineralization in situ. *Am J Dent.* 2013. Vol.26:75-80.
42. Zaze AC, Dias AP, Amaral JG, Miyasaki ML, Sasaki KT, Delbem AC. In situ evaluation of low-fluoride toothpastes associated to calcium glycerophosphate on enamel remineralization. *J Dent.* 2014. Vol.42:1621-1625.
43. Bowen WH. The cariostatic effect of calcium glycerophosphate in monkeys. *Caries Res.* 1972. Vol. 6:43-51.
44. Grenby TH, Bull JM. Protection against dental caries in rats by glycerophosphates or calcium salts or mixtures of both. *Arch Oral Biol.* 1975. Vol. 20:717-724.
45. Grenby TH, Bull JM. Dental caries in laboratory rats from breakfast cereals and its control by a calcium glycerophosphate additive. *Arch Oral Biol.* 1978. Vol.23:675-680.
46. Grenby TH, Bull JM. Use of high-performance liquid chromatography techniques to study the protection of hydroxylapatite by fluoride and glycerophosphate against demineralization in vitro. *Caries Res.* 1980. Vol.14:221-232.
47. Duke SA, Rees DA, Forward GC. Increased plaque calcium and phosphorus concentrations after using a calcium carbonate toothpaste containing calcium glycerophosphate and sodium monofluorophosphate. Pilot study. *Caries Res.* 1979. Vol. 13:57-59.
48. Bao Q, Zhang D, Qi P. Synthesis and characterization of silver nanoparticle and graphene oxide nanosheet composites as a bactericidal agent for water disinfection. *Journal of Colloid and Interface Science.* 2011. Vol. 360: 463-470.
49. Petersen PE. Challenges to improvement of oral health in the 21st century - the approach of the WHO Global Oral Health Programme. *Int Dent J.* 2004. Vol. 54:329-343.
50. Fawole OA, Makunga NP, Opara UL. Antibacterial, antioxidant and tyrosinase-inhibition activities of pomegranate fruit peel methanolic extract. *BMC Complement Altern Med.* 2012. Vol.12:200.
51. Rocha BA, Bueno PC, Vaz MM, Nascimento AP, Ferreira NU, Moreno Gde P, Rodrigues MR, Costa-Machado AR, Barizon EA, Campos JC, de Oliveira PF, Acésio N de O, Martins S de P, Tavares DC, Berretta AA. Evaluation of a Propolis Water Extract Using a Reliable RP-HPLC Methodology and In Vitro and In Vivo Efficacy and Safety Characterisation. *Evid Based Complement Alternat Med.* 2013:670451.
52. Khalili M, Ebrahimzadeh MA, Safdari Y. Antihaemolytic activity of thirty herbal extracts in mouse red blood cells. *Arh Hig Rada Toksikol.* 2014. Vol.65:399-406.
53. Singleton VL, Rossi JA. Colorimetry of total phenolics with phosphomolybdic-phosphotungstic acid reagents. *Am J Enol Vitic.* 1965. Vol. 16:144-158.
54. Turkevich J, Stevenson PC, Hillier J. A study of the nucleation and growth processes in the synthesis of colloidal gold. *Discuss. Faraday Soc.* 1951. Vol. 1: 55-75
55. Gorup LF, Longo E, Leite ER, Camargo ER. Moderating effect of ammonia on particle growth and stability of quasi-monodisperse silver nanoparticles synthesized by the Turkevich method. *J Colloid Interface Sci.* 2011. Vol.15:355-358.
56. Li YF, Guo CJ, Yang JJ, Wei JY, Xu J, Cheng S. Evaluation of antioxidant properties of

- pomegranate peel extract in comparison with pomegranate pulp extract. *Food Chemistry*. 2006. Vol. 96: 254-260.
57. Panichayupakaranant P, Tewtrakul S, Yuenyongsawad S. Antibacterial, anti-inflammatory and anti-allergic activities of standardised pomegranate rind extract. *Food Chemistry*. 2010. Vol.123: 400-403.
 58. Afaq F, Saleem M, Krueger CG, Reed JD, Mukhtar H. Anthocyanin- and hydrolyzable tannin-rich pomegranate fruit extract modulates MAPK and NFkappa B pathways and inhibits skin tumorigenesis in CD-1 mice. *Int J Cancer*. 2005a. Vol.113: 423-433.
 59. Fetrow CW, Avila JR. *The complete guide to herbal medicines*. Simon and Schuster, 2000.
 60. Li J, He X, Li M, Zhao W, Liu L, King X. Chemical fingerprint and quantitative analysis for quality control of polyphenols extracted from pomegranate peel by HPLC. *Food Chemical*. 2015. Vol. 1: 7-11.
 61. Singh M, Jha A, Kumar A, Hettiarachchy N, Rai AK, Sharma D. Influence of the solvents on the extraction of major phenolic compounds (punicalagin, ellagic acid and gallic acid) and their antioxidant activities in pomegranate aril. *J Food Sci Technol*. 2014. Vol. 51:2070-2077.
 62. García-Villalba R, Espín JC, Aaby K, Alasalvar C, Heinonen M, Jacobs G, Voorspoels S, Koivumäki T, Kroon PA, Pelvan E, Saha S, Tomás-Barberán FA. Validated Method for the Characterization and Quantification of Extractable and Nonextractable Ellagitannins after Acid Hydrolysis in Pomegranate Fruits, Juices, and Extracts. *J Agric Food Chem*. 2015. Vol 29:6555-6566.
 63. Arapitsas P Hydrolyzable tannin analysis in food..*Food Chem*. 2012. Vol. 1:1708-1717)
 64. Sathishkumar T , Baskar R, Aravind M, Tilak S, Deepthi S, Bharathikumar VM. Simultaneous Extraction Optimization and Analysis of Flavonoids from the Flowers of *Tabernaemontana heyneana* by High Performance Liquid Chromatography Coupled to Diode Array Detector and Electron Spray Ionization/Mass Spectrometry. *ISRN Biotechnol*. 2012. Vol.18:450948
 65. Miranda M, Fernández A, Lopez-Esteban S, Malpartida F, Moya JS, Torrecillas R. Ceramic/metal biocidal nanocomposites for bone-related applications. *J Mater Sci Mater Med*. 2012. Vol.231655-1662.
 66. Edison TI, Sethuraman MG. Biogenic robust synthesis of silver nanoparticles using *Punica granatum* peel and its application as a green catalyst for the reduction of an anthropogenic pollutant 4-nitrophenol. *Spectrochimica Acta Part A: Molecular and Biomolecular Spectroscopy*. 2013. Vol. 104: 262–264
 67. Meena Kumari M, Jacob J, Philip D. Green synthesis and applications of Au-Ag bimetallic nanoparticles. *Spectrochim Acta A Mol Biomol Spectrosc*.2015. Vol.137:185-192.
 68. Meena Kumari M, Philip D. Degradation of environment pollutant dye using phytosynthesized metal nanocatalysts. *Spectrochim Acta A Mol Biomol Spectrosc*. 2015. Vol. 135:632-638.
 69. Inoue M, In Y, & Ishida T. Calcium binding to phospholipid: structural study of calcium glycerophosphate. *Journal of Lipid Research*, 1992. Vol 33:985.
 70. Xie CM, Lu X, Wang KF, Meng FZ, Jiang O, Zhang HP, Zhi W, Fang LM. Silver nanoparticles and growth factors incorporated hydroxyapatite coatings on metallic implant surfaces for enhancement of osteoinductivity and antibacterial properties. *ACS Appl Mater Interfaces*. 2014. Vol. 6:8580-8589.
 71. Popa CL, Ciobanu CS, Voicu G, Vasile E, Chifiriuc MC, Icinaru SL, Predo D. Influence of Thermal Treatment on the Antimicrobial Activity of Silver-Doped Biological Apatite. *Nanoscale Res Lett*. 2015.10: 502.
 72. Lara HH, Romero-Urbina DG, Pierce C, Lopez-Ribot JL, Arellano-Liménez MJ, Jose-Yacamán M. Effect of silver nanoparticles on *Candida albicans* biofilms na ultrastructural

- study. *J Nanobiotechnology*. 2015. Vol.13:91.
73. Kim KJ, Sung WS, Suh BK, Moon SK, Choi JS, Kim JG, Lee DG. Antifungal activity and mode of action of silver nano-particles on *Candida albicans*. *Biometals*. 2009. Vol. 22:235-242.
 74. Löffler J, Einsele H, Hebart H, Schumacher U, Hrastnik C, Daum G. Phospholipid and sterol analysis of plasma membranes of azole-resistant *Candida albicans* strains. *FEMS Microbiol Lett*. 2000. Vol.185:59-63.
 75. Ordögh L, Vörös A, Nagy I, Kondorosi E, Kereszt A. Symbiotic plant peptides eliminate *Candida albicans* both in vitro and in an epithelial infection model and inhibit the proliferation of immortalized human cells. *Biomed Res Int*. 2014:320796.
 76. Annamalai J, Nallamuthu T. Green synthesis of silver nanoparticles: characterization and determination of antibacterial potency. *Appl Nanosci*. 2016. Vol.6:259-265.
 77. Abdullah NI, Ahmad MB, Shameli K. Biosynthesis of silver nanoparticles using *Artocarpus elasticus* stem bark extract. *Chem Cent J*. 2015. Vol. 9:61.
 78. Khan MN, Khan TA, Khan Z, Al-Thabaiti SA. Green synthesis of biogenic silver nanomaterials using *Raphanus sativus* extract, effects of stabilizers on the morphology, and their antimicrobial activities. *Bioprocess Biosyst Eng*. 2015 . Vol.38:2397-2416.
 79. Bindhu MR , Umadevi M. Silver and gold nanoparticles for sensor and antibacterial applications. *Spectrochim Acta A Mol Biomol Spectrosc*. 2014 . Vol. 128:37-45.
 80. Liu J, Hurt RH. Ion release kinetics and particle persistence in aqueous nano-silver colloids. *Environ Sci Technol*. 2010.Vol. 44:2169-2175.
 81. Feng QL , Wu J, Chen GQ, Cui FZ, Kim TN, Kim JO. A mechanistic study of the antibacterial effect of silver ions on *Escherichia coli* and *Staphylococcus aureus*. *J Biomed Mater Res*. 2000.Vol.52:662-668.
 82. Liu J, Sonshine DA, Shervani S, Hurt RH. Controlled release of biologically active silver from nanosilver surfaces. *ACS Nano*. 2010 Vol.4: 6903-6913.
 83. Lynch RJM, Bebington UK. Calcium glycerophosphate and caries: a review of the literature. *International Dental Journal*. 2004. Vol. 54: 310-314.
 84. Nakashima S. Yoshie M, Sano H, Bahar A. Effect of a test dentifrice containing nano-sized calcium carbonate on remineralization of enamel lesions in vitro. *Journal of Oral Science*. 2009. Vol.51:69-77.

Tables and Figures

Table 1. MIC values of green AgNP and Ag/CaGP, based on dry matter (DM) of the extract obtained by percolation process, phenolic contents, ellagic acid and silver concentration.

<i>C. albicans</i>				
Green Compounds	MIC - DM (mg/g)	MIC - Phenols ($\mu\text{g/mL}$)	MIC - Ellagic Acid ($\mu\text{g/mL}$)	MIC - Ag ($\mu\text{g/mL}$)
Ag/CaGP	0.44	69.4	1.8	156.3
AgNP	0.88	138.8	3.7	312.5
<i>S.mutans</i>				
Ag/CaGP	0.44	69.0	1.8	156.3
AgNP	0.22	35.0	0.9	78.1

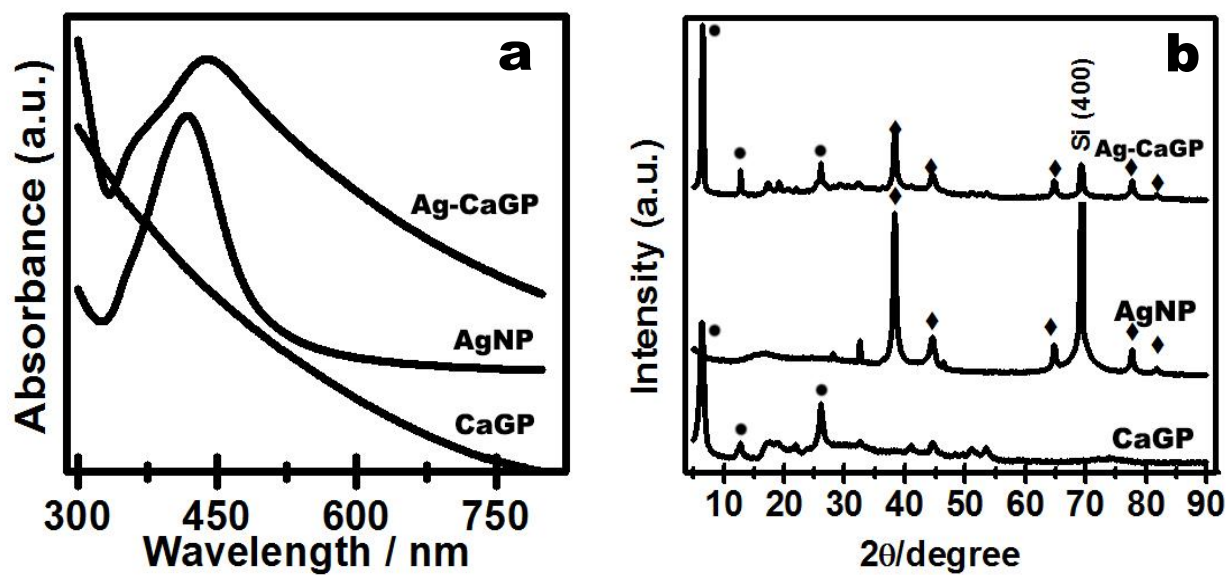


Figure 1. a) UV-Visible spectrum and b) XRD pattern of AgNP and Ag/CaGP and CaGP.

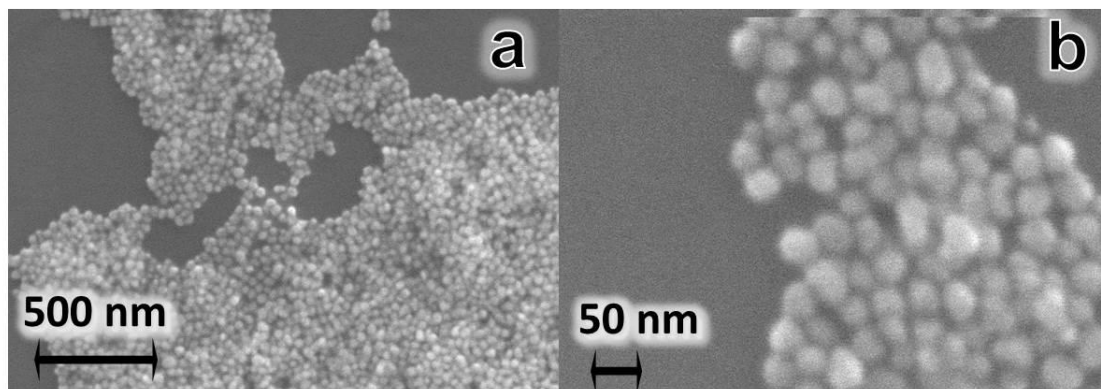


Figure 2. SEM images (a and b) in different magnifications of the AgNP showing size of approximately 50 nm and uniform distribution of this nanoparticles.

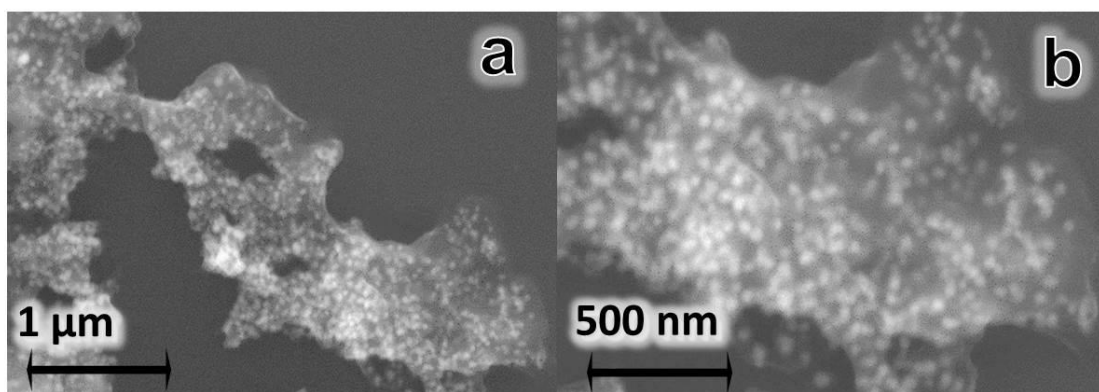


Figure 3. SEM images (a and b) in different magnifications of the Ag/CaGP showing silver nanoparticles in white little spheres dispersed in the bulk of CaGP.

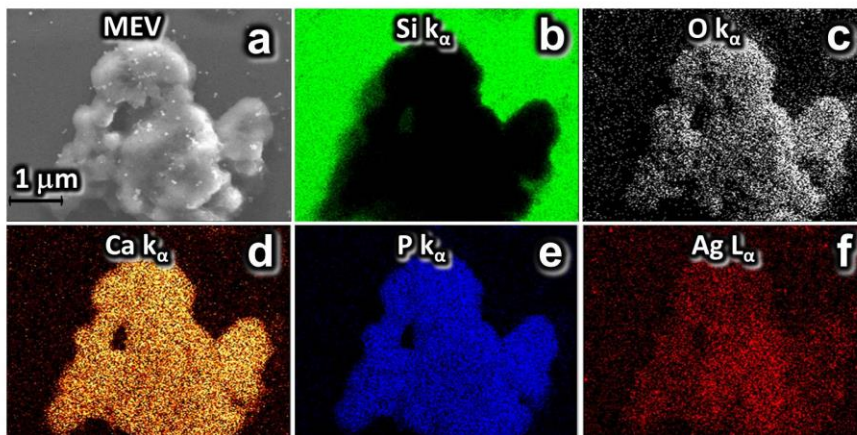


Figure 4. SEM and EDX mapping of the 2D elements issuance Si $K\alpha$, O $K\alpha$, P $K\alpha$, Ca $K\alpha$ and Ag $K\alpha$ false color. Analysis of the distribution of silver nanoparticles in the Ag/CaGP a) SEM image; b) chemical mapping of silicon element present in the substrate where the electron beam was focused showed in green color, and the dark regions of the beam was focused in Ag/CaGP nanocomposite; c-f) oxygen, calcium, phosphorus and silver, respectively, demonstrating they are constituents of the Ag/CaGP.

CAPÍTULO 3

Synthesis and characterization of nanocompounds composed by calcium glycerophosphate and silver nanoparticles reduced by chemical and green route: cytotoxicity analysis

Synthesis and characterization of nanocompounds composed by calcium glycerophosphate and silver nanoparticles reduced by chemical and green route: cytotoxicity analysis

Abstract

In this present study the cytotoxicity of nanobiomaterials composed by silver nanoparticles (AgNP) and calcium glycerophosphate (CaGP) were compared according to its synthesis method: a green route using peel extract of pomegranate and two conventional chemical processes using as reducing agents sodium borohydride (NaBH_4) or sodium citrate ($\text{Na}_3\text{C}_6\text{H}_5\text{O}_7$). The peel extract was obtained by percolation using as solvent ethanol at 70%, and characterized by the quantity of ellagic acid by high performance liquid chromatography and the total phenols expressed in gallic acid by colorimetric method using the Folin-Denis reagent. The green synthesis was then carried out adding the peel extract of pomegranate in a pre-heated aqueous solution (90°C) containing silver nitrate, calcium glycerophosphate (CAS 58409-70-4) previously nanoparticulated by milling for 24 hours and ammonium salt of polymethacrylic acid. For the chemical route, the same reagents were used just varying the reducing agent and solvent, NaBH_4 in isopropanol and $\text{Na}_3\text{C}_6\text{H}_5\text{O}_7$ in deionized water. AgNP synthesized by three methods and without CaGP were used as controls. The nanocompounds were characterized by UV-Vis spectroscopy, X-ray diffraction, and scanning electron microscopy. Metabolic activity of fibroblast cells was quantified by the Alamar Blue assay, after being in contact with each compound at different concentrations (15.6, 31.2, 62.5, 125 and 250 $\mu\text{g}/\text{mL}$) for 24 hours. The viability cell data were analyzed by one-way analysis of variance followed by Bonferroni test ($\alpha=0.05$).

This study proved it was possible to synthesize AgNP in association with CaGP through a green route using pomegranate peel extract. The present route is non-toxic, simple, safe and eco-friendly in comparison with conventional chemical routes. Also, this study compared the cytotoxicity of both AgNP and Ag-CaGP produced by green and chemicals reducers and demonstrated green-

nanocompounds were considerably less toxic. The AgNP synthesized by green route were not toxic in any of the concentrations tested, already for NaBH_4 and $\text{Na}_3\text{C}_6\text{H}_5\text{O}_7$ was cytotoxic at concentrations of 62.5 $\mu\text{g/mL}$. When added to the CaGP, the cytotoxicity of all nanocomposites were reduced, except for the NaBH_4 as the reducing agent in concentrations of the 125 and 250.

Keywords: Nanoparticles, Punicaceae, *Candida albicans*, *Streptococcus mutans*, Celular citotoxicity

Introduction

Nanotechnology is an emerging technology filed [1] with a great impact on human health [2] because the ability of nanotherapeutics to provide targeted drug delivery [3], extend drug half-life [4], improve drug solubility [5] and drug's therapeutic index [6,7], as well as to reduce drug's immunogenicity [8] which has resulted in a potential to revolutionize the treatment of many diseases [2,9].

Silver nanoparticles (AgNP) have been reported in multiple uses of biomedical applications [10] for their effectiveness against a broad spectrum of microorganisms [11]. Several approaches have been employed for its synthesis, including chemical reduction by sodium borohydride [12;13], sodium citrate [14;15] and biogenic routes [16-18]. Although chemical routes may produce AgNP in large amounts and shorter time, it often requires more energy and the use of costly and hazardous reagents. Current strategies of green synthesis include the use of biodegradable polymers and environmentally non-toxic solvents like plant extracts [19]. Many substances present in the majority of plants, including carbohydrates and bioactive compounds belonging to the phenolic, flavonoid, alkaloid and terpenoid families may play an important role in the green mechanisms of metallic nanoparticles synthesis [20].

Punica granatum is a relatively non-toxic plant [21] generally known as pomegranate that belongs to *Punicaceae* family [22]. Pomegranate peel extract is rich in polyphenols which are composed of ellagic acid derivatives such as the ellagitannins, punicalagin and punicalin, gallic acid and ellagic acid, and it has been reported to present antioxidant and antimicrobial properties [23]. In addition, these phytochemicals would be related to the stability of AgNPs [10,24] by the reduction of aqueous Ag^+ ions in Ag^0 [25-27] as well as the increase of the biocompatibility of the green synthesized nanoproducts [20].

Thinking of the AgNP antimicrobial potential and the inherent biocompatible nature of phytochemicals involved in the green synthesis, its association with calcium phosphates would

encourage the development of nanocompounds to prevent dental caries and stimulate remineralization process. Miranda et al. [28] synthesized a nanocompound containing AgNP and hydroxyapatite using sodium borohydride to reduce Ag^+ from AgNO_3 to Ag^0 . This compound was effective against a gram-negative (*Escherichia coli*) and a gram-positive (*Micrococcus luteus*) bacteria, but its effectiveness was reduced when tested against a fungus (*Issatchenkia orientalis*). Other calcium phosphates, such as calcium glycerophosphate (CaGP), have also been investigated due to its potential in the treatment of dental lesion caries [29-32]. It is an organic salt of phosphate (CaGP) with cariostatic properties [29;30] for reducing the enamel acid-dissolution through buffering the pH of dental biofilm, decreasing its mass and modifying its metabolism, as well as elevating the calcium and/or phosphorus levels in the dental biofilm [33;34].

Development and applications of new biomaterials involve important steps that should not be ignored, such as carrying out biocompatibility tests, these may be quantitative or qualitative, in vitro or in vivo, involving human cell lines.

In this article, synthesis and characterization of a nanomaterial containing silver nanoparticles reduced by two different routes were approached, focusing in the cytotoxicity of this new compound against fibroblast cells.

Material and Methods

Pomegranate peel extracts

This study was performed on peels of pomegranate fruit which was bought from a local supermarket in São Paulo (CEAGESP – Company Warehouses and General Warehouses of São Paulo). The fruits were cultivated in the northeastern part of the State of São Paulo and harvested in May of 2015. A specimen of the plant drug was deposited in the Herbarium of the University of São Paulo, Ribeirão Preto, SP, Brazil. Pomegranates were washed with water and manually peeled. The peels were dried in an incubator at 50°C, and grounded into powder form using a blender [37]. The powder was then filtered through a 42-mesh sieve to obtain standardized particle size [38].

The powder of the peels was submitted to an extraction with ethanol at 70% by maceration and percolation process [39]. This method was selected based on the quantification of ellagic acid and phenolic compounds obtained previously.

Synthesis of AgNP and Ag-CaGP: Chemical and Green routes

Nanocomposites Ag-CaGP/chemicals and Ag-CaGP/green were synthesized in Interdisciplinary Laboratory of Electrochemistry and Ceramics of the Chemistry (LIEC) Department of Chemistry, Federal University of São Carlos (UFSCar), São Carlos, Brazil. Initially, the commercial form of calcium glycerophosphate (CaGP) (β -isomer 80% and 20% of rac- α -isomer, CAS 58409-70-4, Sigma-Aldrich Chemical Co., St. Louis, Missouri, USA) was nanoparticulated using a ball mill for 24 hours at 120 rpm. Then, three methods were used to synthesize the Ag-CaGP, based on the reduced agent of silver ions: i) sodium borohydride (NaBH_4 , Sigma-Aldrich); ii) sodium citrate ($\text{Na}_3\text{C}_6\text{H}_5\text{O}_7$, Merck KGaA, Darmstadt, Germany) and iii) pomegranate peels.

The synthesis using the reducing agent NaBH_4 was based on the methodology proposed by Miranda et al. [28] Suspensions containing CaGP and silver nitrate (AgNO_3 , Merck KGaA) were prepared in the presence of a surfactant, ammonium salt of polymethacrylic acid, ((NH-PM),

Polysciences Inc., Warrington, PA, USA) and using isopropanol as solvent. Then, NaBH_4 was added into the suspension for reducing the Ag ions to silver nanoparticles (AgNP). The molar stoichiometric ratio between Ag^+ and NaBH_4 was 1:1.26, respectively. The second chemical route to prepare the nanocomposite Ag-CaGP was based on Turkevich et al. [40] and Gorup et al. [41] with some modifications. The reducing agent of Ag ions from AgNO_3 was $\text{Na}_3\text{C}_6\text{H}_5\text{O}_7$, and the stoichiometric ratio of each compound was 1:3. 0.85 g of AgNO_3 was added into 100 mL of deionized water, followed by 5 g CaGP and 0.5 mL of NH-PM. This solution was kept under magnetic stirring and heating until reaching 95°C . The yellow color of the solution indicated the formation of AgNP

For the Ag-CaGP/green nanocomposite synthesis, pomegranate peels extract (0.070 g) previously obtained was added into a solution of CaGP (0.25 g) and AgNO_3 (0.042 g). Following 0.025 ml of NH-PM was added, totalizing a final volume of 10 mL. This solution was kept under agitation and until the temperature reaches 95°C when it became amber indicating the formation of AgNP. Controls containing only the respective reducing agents and surfactant, AgNO_3 , ellagic acid, CaGP and bulk peel extract were used (Table 1).

Characterization of Ag-CaGP nanocomposites

In order to evaluate the formation of AgNP associated or not with CaGP, the UV-Vis (spectrophotometer Shimadzu MultiSpec-1501, Shimadzu Corporation, Tokyo, Japan) absorption spectroscopy technique was employed and X-ray diffraction (XRD) (Diffractometer Rigaku DMax-2000PC, Rigaku Corporation, Tokyo, Japan). Also, the particles morphology was characterized by scanning electron microscopy (SEM) on a Zeiss Supra 35VP microscope (S-360 microscope, Leo, Cambridge, USA) with field emission gun electron effect (FEG-SEM) operating at 10 kV.

Evaluation of nanocomposites Ag-CaGP/Chemical and Ag-CaGP/Green in cell culture

Lineage and cell culture

The L929 fibroblast cells line was purchased from the Cell Bank of Rio de Janeiro (BCRJ). The cells were cultured in DMEM culture medium (Gibco[®]) (supplemented with 1% (v/v) of an antibiotic solution (Sigma[®]) containing 100 U/mL of penicillin, 100 µg/mL of streptomycin and 25 µg/mL of amphotericin B), and 10% (v/v) of fetal bovine serum (FBS) (Gibco[®]). The cells were maintained in an incubator at 37°C and an atmosphere of 5% CO₂. Cells were subcultured every 5-7 days using 0.9% saline solution to wash them, and 0.25% of Trypsin-EDTA (Sigma[®]) to disaggregate them bottle. After breakout, these cells were centrifuged at 1000 rpm for 10 minutes at 10°C, re-suspended in DMEM (supplemented with FBS), and cells were counted using a Neubauer chamber.

Cytotoxicity of nanocomposites Ag-CaGP/Chemicals and Ag CaGP/Green

Cell viability was measured by Alamar Blue assay based on the experimental protocol described by Kuete et al. [42] where, basically, the metabolically active cells reduce the corant resazurin to resorufin which become highly fluorescent [42]. For that, sub-cultured fibroblast cells from the 3rd to 8th passages were seeded in 96-well microplate at a density of 0.5×10^5 cells/well. After 24 hours, 20 µL of each dilution of the nanocomposites Ag-CaGP/Chemical or Ag-CaGP/Green (from 250 to 15 µg/mL), as well as of AgNP synthesized by conventional and green routes, were added into the wells containing fibroblast cells in medium without FBS. These concentrations were based on the minimum inhibitory concentration (MIC) of silver obtained in previous studies (data not published yet). 24 hours after treatment, the medium was removed, cells were washed with saline (0.9%), and 20 µL of resazurin (Sigma-Aldrich) 0.01% (w/v) in deionised water were added into each well containing 180 µL of DMEM supplemented with 10% FBS Then the plate was incubated in an incubator at 37°C for 4 hours. After this period, the fluorescence was

measured at 540 and 590 nm for excitation and emission, respectively, in a plate fluorometer (BioTek Synergy 2 - Multi-mode microplate reader, BioTek Instruments Inc., USA). The data were expressed as percentage of cell viability.

Statistical Analysis

The experiments were conducted at triplicate in three different occasions, and data were analyzed by One-way analysis of variance followed by BonFerroni test and statistically significant differences were set at $p < 0.05$.

Results

Characterization of Ag-CaGP nanocomposites

AgNP were formed using both chemical reducing agents ($\text{Na}_3\text{C}_6\text{H}_5\text{O}_7$ and NaBH_4) and pomegranate peel extract, with or without the addition of CaGP. UV-Vis absorption spectroscopy showed that all Ag-CaGP compounds presented silver with nanosize with the presence of an intense absorption peak, denominated plasmon band which occurred between 420 and 450 nm (Figure 1a). Figure 1a also presented the UV-Vis of AgNP and CaGP, showing CaGP did not exhibit absorption peak in the visible region of the electromagnetic spectrum. XRD pattern demonstrated all Ag-CaGP nanocompounds are composed of metal silver particles and CaGP (Figure 1b). The typical powder XRD patterns for AgNP and CaGP are shown in Figure 1b. AgNP presented diffraction peaks at $2\theta = 38.2^\circ, 44.4^\circ, 64.6^\circ, 77.5^\circ,$ and 81.7° , which can be indexed to (111), (200), (220), (311), and (222) planes of pure silver with face-centered cubic system (PDF № 04-0783). Data from CaGP showed diffraction peaks at $2\theta = 6.30^\circ, 12.3^\circ, 26.4^\circ, 41.1^\circ,$ and 44.2° and the corresponding crystallographic form (PDF № 1-17) [43].

SEM images of Ag-CaGP synthesized by chemical routes demonstrated that silver nanoparticles decorated the surface of CaGP (Figure 2a and 2b) While in the images of Ag-CaGP produced by green route silver nanoparticles seemed to be involved by a “matrix” of CaGP (Figure 2c).

Cytotoxicity evaluation of nanocomposites Ag-CaGP/Chemical and Ag-CaGP/Green in cell culture of fibroblasts

The cytotoxicity of fibroblasts treated with different concentrations (250-15 $\mu\text{g}/\text{mL}$) of each nanocomposite Ag-CaGP/Chemical and Ag-CaGP/Green was expressed by the percentage of viable cells compared to the control (100% of cellular viability). Among three of the nanocomposites tested (Ag-CaGP/C, Ag-CaGP/B, Ag-CaGP/E), there was a reduction of the cellular viability just for the

Ag-CaGP/B nanocomposite at 125 and 250 $\mu\text{g}/\text{mL}$ concentrations (Figure 3).

For AgNP synthesized without CaGP by green route (AgNP/E), the cytotoxicity was remarkably reduced when compared with AgNP synthesized conventionally by NaBH_4 (AgNP/B) and $\text{Na}_3\text{C}_6\text{H}_5\text{O}_7$ (AgNP/C), with significant reduction of cell viability at concentrations above 62.5 $\mu\text{g}/\text{mL}$ (Figure 4). While for AgNP/B the cell viability started to be significantly reduced from 31.2 $\mu\text{g}/\text{mL}$, and for AgNP ($\text{Na}_3\text{C}_6\text{H}_5\text{O}_7$) all the concentrations tested were as toxic as DMSO at 10%. Comparing these AgNP among them in each concentration, again AgNP/E showed significantly lower cytotoxicity than the other nanoparticles (Figure 4).

Comparing controls tested (Figure 5) CaGP, NaBH_4 and $\text{Na}_3\text{C}_6\text{H}_5\text{O}_7$ did not exhibit any significant reduction in cell viability. Nevertheless, AgNO_3 was as toxic as DMSO at 10% regardless of the concentration. Pomegranate peel extract presented significant reduction of cell viability at concentration from 62.5 $\mu\text{g}/\text{mL}$, and ellagic acid from 31.2 $\mu\text{g}/\text{mL}$.

Discussion

The present study aimed to synthesize Ag-CaGP by two conventional chemical routes using $\text{Na}_3\text{C}_6\text{H}_5\text{O}_7$ and NaBH_4 as reducing agents, and a green route through pomegranate peel extract. The formation of AgNP by reduction of Ag^+ from AgNO_3 in a solution containing CaGP was evidenced by color change of the reaction mixture. According Ahmad et al. [44] this color change is due to the surface plasmon resonance of the metal nanoparticles. In general and similarly with previous studies [45-48], dark brown color was showed in the compounds after the formation of AgNP by peel pomegranate extract, regardless of the presence of CaGP. The plasmon band resulted from the collective excitation of the free electrons of the silver particles at the surface of the nanoparticle, which is known as surface plasmon absorption, and in our study it ranged of about 420 nm to 470 nm. The absorption maxima increased when AgNP was associated to CaGP, except for the Ag-CaGP synthesized by NaBH_4 . It could be related to the size distribution of the silver particles [10] in the different compounds, which, although tests to prove it had not been carried out, can be noted by the SEM images of AgNP and Ag-CaGP.

Pomegranate peel extract used as reducing agent expressively diminished the cytotoxicity of silver nanoparticles with or not in association with CaGP. More interestingly the addition of CaGP to AgNP suppressed the toxicity of silver nanoparticles for the compounds synthesized by both routes (green and chemical) and in all concentrations tested, except when NaBH_4 was used as reducing agent at the highest concentrations (125 and 250 $\mu\text{g}/\text{mL}$). One of the explanations for that is once AgNP associated with CaGP could not interact with phospholipids of the plasmatic membrane of fibroblast cell, and consequently it would not lead the cellular death caused by the disruption of membrane. Also, the AgNP penetration via cellular membrane would be impaired avoiding the mechanism of action of silver inside the cell. Moreover, AgNP with CaGP would reduce the production of the reactive oxygen species (ROS) promoted by the AgNP alone, which in biological systems at higher concentrations would lead to oxidative damages to proteins, lipids and DNA

[49,50].

Several studies have presented AgNP synthesized by physical or chemical routes have the potential to induce significant toxicity to cells and animals [51-53]. Results from our study agree with them since AgNP synthesized using $\text{Na}_3\text{C}_6\text{H}_5\text{O}_7$ was considerably toxic to fibroblast cells, being the percentage of cell viability similar to DMSO even at lower concentrations. The other chemical route using NaBH_4 was also toxic to fibroblast cells, but at concentrations above $31.2 \mu\text{g/mL}$. It might be that $\text{Na}_3\text{C}_6\text{H}_5\text{O}_7$ reducing agent has not been as efficient as NaBH_4 and higher concentration of Ag^+ was lasting in the AgNP solution. This supposition could be supported by the similar cytotoxicity found by AgNO_3 . Pursuing the rationale of cytotoxicity of AgNP, silver ions also would induce the ROS and oxidative stress in the cells [55] as well as could react with negative charge on the cell membrane surface causing its disruption and apoptosis. In contrast, AgNP produced using pomegranate peel extract allowed cellular viability more than 70% even at the highest concentration ($250 \mu\text{g/mL}$). These results are similar to those found by Amooaghaie et al [10], where AgNP synthesized by conventional method with were eleven-fold more toxic when compared to AgNP produced using *Nigella sativa* at a concentration of $0.2\text{mg} / \text{L}$. Ahamed et al. [44] evaluated the biological response of AgNP produced from tooth to garlic clove extract, and noted that there was no damage to the cell membrane and also no production of significant ROS, maintaining the cell viability of human lung epithelial cells similar with the positive control. As above studies our green results demonstrated AgNP synthesized by peel extract of pomegranate presented more biocompatibility than AgNP produced by conventional chemical routes, and it might be due the non-toxic coating promoted by this extract [10].

Moreover, our results also demonstrated it was possible to associate two different compounds, a nanoparticulated metal and a salt of organic calcium phosphate, by a green route to produce a nanocompound of Ag-CaGP lesser cytotoxic than Ag-CaGP chemically synthesized using NaBH_4 , even at the highest silver concentration. On the other hand, Ag-CaGP produced using

$\text{Na}_3\text{C}_6\text{H}_5\text{O}_7$ reducing agent did not interfere on the percentage of cellular viability being similar to both the positive control (100% of viable cells) and the Ag-CaGP greenly synthesized. This results are not in agreement when AgNP were synthesized without CaGP and using the same chemical routes, where AgNP- $\text{Na}_3\text{C}_6\text{H}_5\text{O}_7$ was as cytotoxic as negative control (10% DMSO). There is not a plausible explanation for that, and further investigations are very recommended to understand the role of each silver reducing agent in the presence or not of other substances.

In conclusion, this study proved it was possible to synthesize AgNP in association with CaGP through a green route using pomegranate peel extract. The present route is non-toxic, simple, safe and eco-friendly in comparison with conventional chemical routes. Also, this study compared the cytotoxicity of both AgNP and Ag-CaGP produced by green and chemicals reducers and demonstrated green-nanocompounds were considerably less toxic and safer, opening up an opportunity to create a promising biomaterial with dental and medical application in the near future.

Acknowledgements:

This study was supported by: São Paulo Research Foundation (FAPESP, Process 2013/24200-9 and 2014/08648-2), Brazil; and Coordination for the Improvement of Higher Education Personnel (Capes, Process 88887.068358/2014-00 and 88881.030445/2013-01), Brazil.

References:

1. Hussain I, Singh NB, Singh A, Singh H, Singh SC. Green synthesis of nanoparticles and its potential application. *Biotechnology Lett.* 2015:1-16
2. Hafner A, Lovrić J, Lakoš GP, Pepić I. Nanotherapeutics in the EU: an overview on current state and future directions. *International Journal of Nanomedicine.* 2014. Vol.9:1005-1023.
3. Brown PK, Qureshi AT, Moll AN, Hayes DJ, Monroe WT. Silver Nanoscale Antisense Drug Delivery System for Photoactivated Gene Silencing. 2013. Vol. 7: 2948-2959.
4. Hou H, Nieto A, Ma F, Freeman WR, Sailor MJ, Cheng L. Tunable sustained intravitreal drug delivery system for daunorubicin using oxidized porous silicon. *Journal of Controlled Release.* 2014. Vol. 28: 46-54.
5. Firooz A, Nafisib S, Maibachc HI. Novel drug delivery strategies for improving econazole antifungal action. *International Journal of Pharmaceutics.* 2015. Vol. 495: 599-607.
6. Guan Q, Sun S, Li X, Lv S, Xu T, Sun J, Feng W, Zhang L, Li Y. Preparation, in vitro and in vivo evaluation of mPEG-PLGA nanoparticles co-loaded with syringopicroside and hydroxytyrosol. *Journal of Materials Science: Materials in Medicine - Springer.* 2016. 27:1-13.
7. Tian X, Lara H, Wagner KT, Saripalli S, Hyder SN, Foote M, Sethi M, Wang E, Caster JM, Zhang L, Wang AZ. Improving DNA double-strand repair inhibitor KU55933 therapeutic index in cancer radiotherapy using nanoparticle drug delivery. *Nanoscale.* 2015. Vol.7: 20211-20219.
8. Tian Y, Suping L, Song J, Tianjiao J, Zhu Motao, Anderson GJ, Wei J, Nie G. A doxorubicin delivery platform using engineered natural membrane vesicle exosomes for targeted tumor therapy. *Biomaterials.* 2014. Vol. 35: 2383-2390.
9. Petros RA, DeSimone JM. Strategies in the design of nanoparticles for therapeutic applications. *Nature Reviews Drug Discovery.* 2010. Vol.9:615-627.
10. Amooaghaie R, Saeri MR, Azizi M. Synthesis, characterization and biocompatibility of silver nanoparticles synthesized from *Nigella sativa* leaf extract in comparison with chemical silver nanoparticles. *Ecotoxicol Environ Saf.* 2015. Vol. 120:400-408.
11. Ge L, Li Q, Wang M, Ouyang J, Li X, Xing MM. Nanosilver particles in medical applications: synthesis, performance, and toxicity. *International Journal Nanomedicine.* 2014. Vol. 9:2399-2407.
12. Mallin MP, Murphy CJ. Solution-Phase Synthesis of Sub-10 nm Au-Ag Alloy Nanoparticles. *Nano Letters.* 2002. Vol. 2:1235-1237.
13. Kometani N, Tsubonishi M, Fujita T, Asami K, Yonezawa. Preparation and Optical Absorption Spectra of Dye-Coated Au, Ag, and Au/Ag Colloidal Nanoparticles in Aqueous Solutions and in Alternate Assemblies. *Langmuir.* 2001. Vol. 17: 578-580
14. Link S, Wang ZL, Sayed MA. Alloy Formation of Gold–Silver Nanoparticles and the Dependence of the Plasmon Absorption on Their Composition. *J. Phys. Chem. B.* 1999. Vol.103: 3529-3533.
15. Sánchez-Ramírez JF, Pal U, Hernández-Nolasco L, Mendoza-Álvarez J, Pescador-Rojas JÁ. Synthesis and Optical Properties of Au-Ag Alloy Nanoclusters with Controlled Composition. *Journal of Nanomaterials.* 2008. 620412.
16. U.S. EPA. Nanomaterial Case Study: Nanoscale Silver in Disinfectant Spray (Final Report), U.S. Environmental Protection Agency, Washington, DC (2012) EPA/600/R-10/081F.
17. Liu H, Sun K, Zhao J, Guo R, Shen M, Cao X, Zhang G, Shi X. Dendrimer-mediated synthesis and shape evolution of gold–silver alloy nanoparticles. *Colloids and Surfaces A: Physicochemical and Engineering Aspects.* 2012. Vol 405: 22-29.
18. Tamuly C, Hazarika M, Borah SCh, Das MR, Boruah MP. In situ biosynthesis of Ag, Au and

- bimetallic nanoparticles using Piper pedicellatum C.DC: Green chemistry approach. *Colloid Surfaces B*. 2013. Vol 102: 627-634.
19. da Camara DM, Pessan JP, Francati TM, Souza JA, Danelon M, Delbem AC. Fluoride toothpaste supplemented with sodium hexametaphosphate reduces enamel demineralization in vitro. *Clin Oral Investig*. 2016.
 20. Das RK, Brar SK. Plant mediated green synthesis: modified approaches. *Nanoscale*. 2013. Vol. 5: 10155-10162.
 21. Patel C, Dadhaniya P, Hingorani L, Soni MG. Safety assessment of pomegranate fruit extract: Acute and subchronic toxicity studies. *Food and Chemical Toxicology*. 2008. Vol. 46: 2728-2735.
 22. Edison TJ, Sethuraman MG. Biogenic robust synthesis of silver nanoparticles using Punica granatum peel and its application as a green catalyst for the reduction of an anthropogenic pollutant 4-nitrophenol. *Spectrochim Acta A Mol Biomol Spectrosc*. 2013. Vol. 104:262-264.
 23. Ganeshkumar M, Sathishkumar M, Ponrasu T, Dinesh MG, Suguna L. Spontaneous ultra fast synthesis of gold nanoparticles using Punica granatum for cancer targeted drug delivery. *Colloids Surf B Biointerfaces*. 2013.106:208-216.
 24. Park Y. A new paradigm shift for the green synthesis of antibacterial silver nanoparticles utilizing plant extracts. *Toxicol*. 2014. Vol. 30:169-178
 25. Ahmad N, Sharma S, Rai R. Rapid green synthesis of silver and gold nanoparticles using peels of Punica granatum. *Advanced Materials Letters*. 2012. Vol. 3:376-380.
 26. Meena Kumari M, Jacob J, Philip D. Green synthesis and applications of Au-Ag bimetallic nanoparticles. *Spectrochim Acta A Mol Biomol Spectrosc*.2015. Vol.137:185-19
 27. Meena Kumari M, Philip D. Degradation of environment pollutant dye using phytosynthesized metal nanocatalysts. *Spectrochim Acta A Mol Biomol Spectrosc*. 2015. Vol. 135:632-638.
 28. Miranda M, Fernández A, Lopez-Esteban S, Malpartida F, Moya JS, Torrecillas R. Ceramic/metal biocidal nanocomposites for bone-related applications. *J Mater Sci Mater Med*. 2012. Vol.231655-1662.
 29. do Amaral JG , Sasaki KT, Martinhon CC, Delbem AC. Effect of low-fluoride dentifrices supplemented with calcium glycerophosphate on enamel demineralization in situ. *Am J Dent*. 2013. Vol26:75-80.
 30. Zaze AC, Dias AP, Amaral JG , Miyasaki ML , Sasaki KT , Delbem AC. In situ evaluation of low-fluoride toothpastes associated to calcium glycerophosphate on enamel remineralization. *J Dent*. 2014. Vol.42:1621-1625.
 31. da Camara DM, Pessan JP, Francati TM, Souza JA, Danelon M, Delbem AC. Fluoride toothpaste supplemented with sodium hexametaphosphate reduces enamel demineralization in vitro. *Clin Oral Investig*. 2016.
 32. do Amaral JG, Delbem AC, Pessan JP, Manarelli MM, Barbour ME. Effects of polyphosphates and fluoride on hydroxyapatite dissolution: A pH-stat investigation. *Arch Oral Biol*. 2016. 63:40-46
 33. Lynch RJM, Bebington UK. Calcium glycerophosphate and caries: a review of the literature. *International Dental Journal*. 2004. Vol. 54: 310-314.
 34. Nakashima S, Yoshie M, Sano H, Bahar A. Effect of a test dentifrice containing nano-sized calcium carbonate on remineralization of enamel lesions in vitro. *Journal of Oral Science*. 2009. Vol.51:69-77.
 35. Vega-Villa KR, Takemoto JK, Yáñez JA, Remsberg CM, Forrest ML, Davies NM. Clinical toxicities of nanocarrier systems. *Adv Drug Deliv Rev*. 2008. Vol.6:929-938.
 36. Nel A, Xia T, Mädler L, Li N. Toxic potential of materials at the nanolevel. 2006. *Science*. Vol. 311:622-627.

37. Fawole OA, Makunga NP, Opara UL. Antibacterial, antioxidant and tyrosinase-inhibition activities of pomegranate fruit peel methanolic extract. *BMC Complement Altern Med.* 2012. Vol.12:200.
38. Rocha BA, Bueno PC, Vaz MM, Nascimento AP, Ferreira NU, Moreno Gde P, Rodrigues MR, Costa-Machado AR, Barizon EA, Campos JC, de Oliveira PF, Acésio N de O, Martins S de P, Tavares DC, Berretta AA. Evaluation of a Propolis Water Extract Using a Reliable RP-HPLC Methodology and In Vitro and In Vivo Efficacy and Safety Characterisation. *Evid Based Complement Alternat Med.* 2013:670451.
39. Khalili M, Ebrahimzadeh MA, Safdari Y. Antihaemolytic activity of thirty herbal extracts in mouse red blood cells. *Arh Hig Rada Toksikol.* 2014. Vol.65:399-406.
40. Turkevich J, Stevenson PC, Hillier J. A study of the nucleation and growth processes in the synthesis of colloidal gold. *Discuss. Faraday Soc.* 1951. Vol.1: 55-75
41. Gorup LF, Longo E, Leite ER, Camargo ER. Moderating effect of ammonia on particle growth and stability of quasi-monodisperse silver nanoparticles synthesized by the Turkevich method. *J Colloid Interface Sci.* 2011. Vol.360:355-358.
42. Kuete V, Wiench B, Alsaid MS, Alyahya MA, Fankam AG, Shahat AA, Efferth T. Cytotoxicity, mode of action and antibacterial activities of selected Saudi Arabian medicinal plants. *BMC Complement Altern Med.* 2013. Vol.13:354.
43. Inoue M, In Y, & Ishida T. Calcium binding to phospholipid: structural study of calcium glycerophosphate. *Journal of Lipid Research*, 1992. Vol 33:985.
44. Ahmad N, Sharma S, Alam MK, Singh VN, Shamsi SF, Mehta BR, Fatma A. Rapid synthesis of silver nanoparticles using dried medicinal plant of basil. *Colloids Surf B Biointerfaces.* 2010 Vol.81:81-86
45. Chitra G, Balasubramani G, Ramkumar R, Sowmiya R, Perumal P, Mukia maderaspatana (Cucurbitaceae) extract-mediated synthesis of silver nanoparticles to control *Culex quinquefasciatus* and *Aedes aegypti* (Diptera: Culicidae), *Parasitol. Res.* 2015. Vol 114:1407-1415.
46. Singh M, Kalaivani R, Manikandan S, Sangeetha N, Kumaraguru AK. Facile green synthesis of variable metallic gold nanoparticle using *Padina gymnospora*, a brown marine macro alga. *Appl. Nanosci.* 2012. Vol. 3:145-151.
47. Huang, Q. Li, D. Sun, Y. Lu, Y. Su, X. Yang, H. Wang, Y. Wang, W. Shao, N. He, J. Hong, C. Chen, Biosynthesis of silver and gold nanoparticles by novel sundried *Cinnamomum camphora* leaf. *Nanotechnology.* 2007.105104 (11pp).
48. Chantini AB, Balasubramani G, Ramkumar R, Sowmiya, Balakumaran MD, Kalaichelvan PT, Perumal P. Structural characterization, antioxidant and in vitro cytotoxic properties of seagrass, *Cymodocea serrulata* (R.Br.) Asch. & Magnus mediated silver nanoparticles. *Journal of Photochemistry and Photobiology B: Biology.* 2015. Vol 153. 145-152.
49. Rushton EK, Jiang J, Leonard SS, Eberly S, Castranova V, Biswas P, Elder A, Han X, Gelein R, Finkelstein J, Oberdörster G. Concept of assessing nanoparticle hazards considering nanoparticle dose-metric and chemical/biological response metrics. *J Toxicol Environ Health A.* 2010. Vol.73:445-461.
50. Kaur J, Tikoo K. Evaluating cell specific cytotoxicity of differentially charged silver nanoparticles. *Food Chem Toxicol.* 2013. Vol. 51:1-14.
51. Abou El-Nour K M, Eftaiha A, Al-Warthan A, Ammar R A. Synthesis and applications of silver nanoparticles. *Arab. J. Chem.* 2010. Vol. 3:135-140
52. AshaRani P, Low Kah Mun G, Hande M P, Valiyaveetil S. Cytotoxicity and genotoxicity of silver nanoparticles in human cells. *ACS Nano.* 2008. Vol. 3: 279-290.
53. Chou K-S and Ren C-Y Synthesis of nanosized silver particles by chemical reduction method. *Mater. Chem. Phys.* 2000. Vol. 64:241-246

54. Haase A, Manton A, Graf P, Plendl J, Thuenemann A, Meier W, Taubert A, Luch A. A novel type of silver nanoparticles and their advantages in toxicity testing in cell culture systems Arch. Toxicol. 2012. Vol.86 1089-1098
55. Hatipoglu MK, Keleştemur S, Altunbek M, Culha M. Source of cytotoxicity in a colloidal silver nanoparticle suspension. Nanotechnology. 2015. Vol. 26:195103.

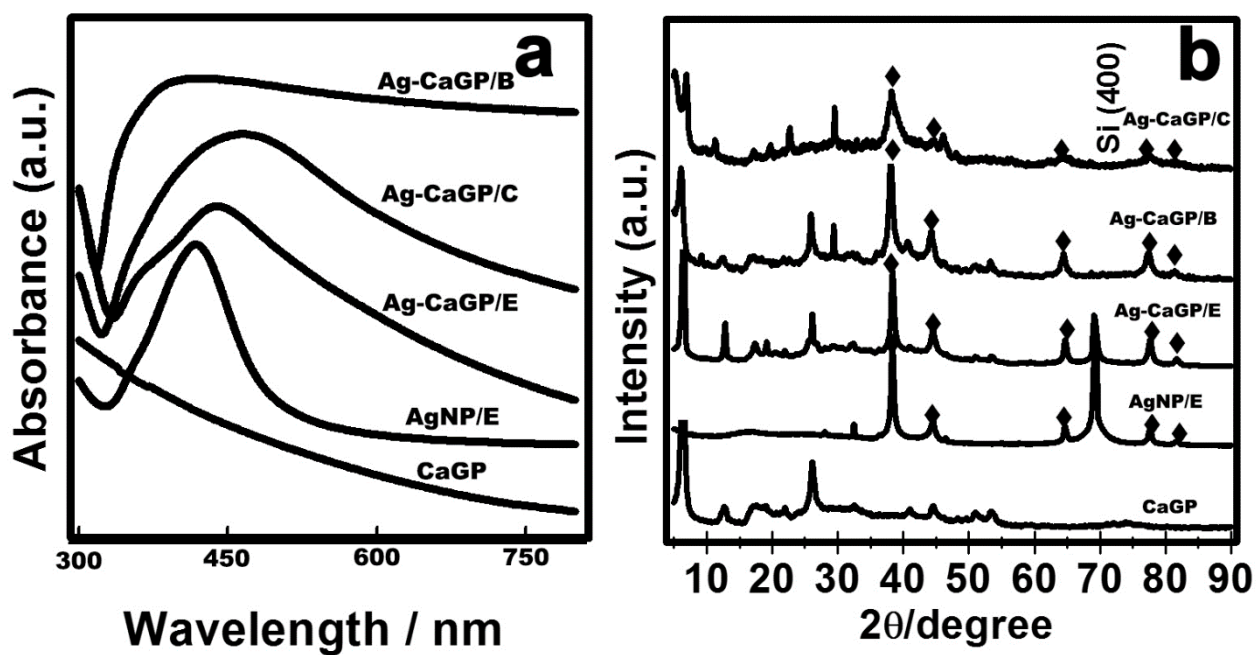


Figure 1. a) UV-Visible spectrum and b) XRD pattern samples Ag-CaGP/B; Ag-CaGP/C; Ag-CaGP/E; AgNP/E and CaGP.

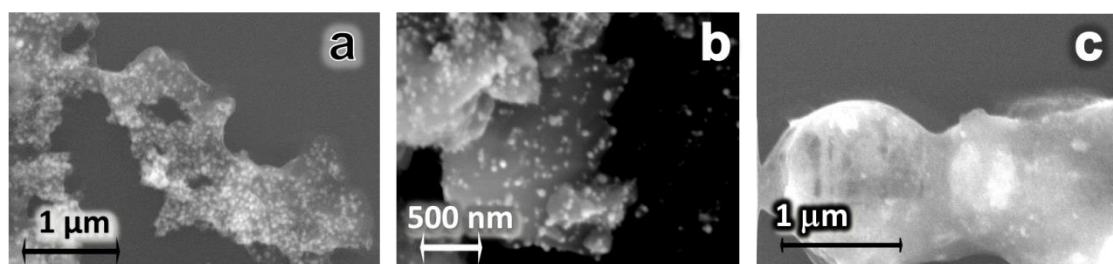


Figure 2. SEM images of the nanocompounds: a) Ag-CaGP/E; b) Ag-CaGP/B; c) Ag-CaGP/C.

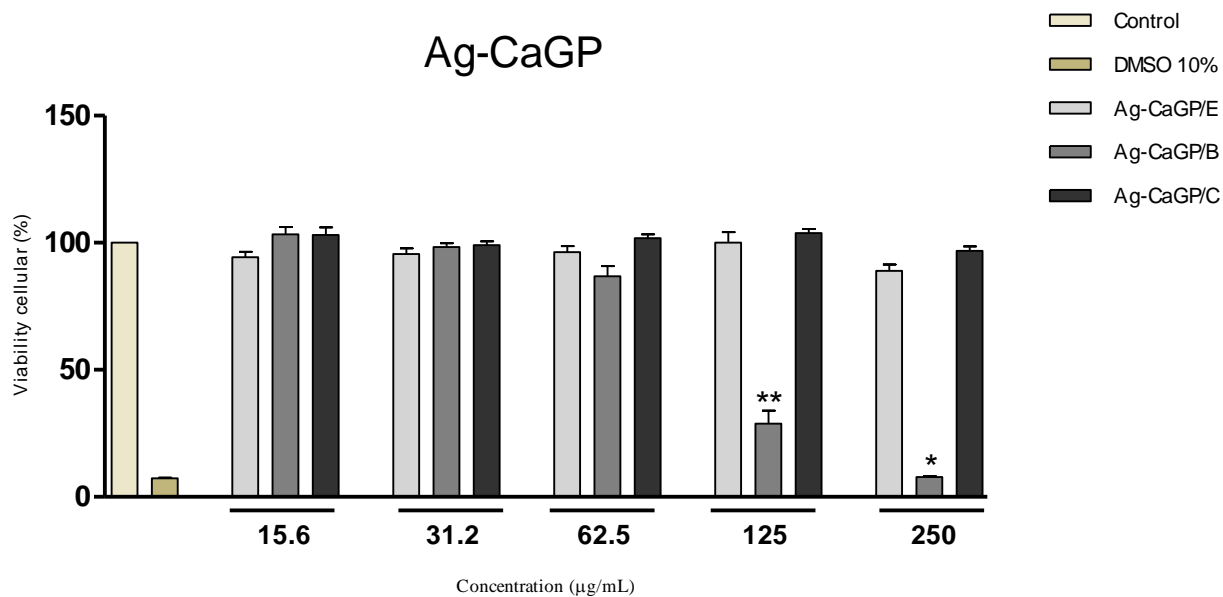


Figure 3. Cell Cytotoxicity obtained by Alamar Blue assay for compounds Ag-CaGP/E; Ag-CaGP/B; Ag-CaGP/C in L929 fibroblast cells. * Indicates statistical differences between the concentration tested and positive control (100% viable cells) and ** indicates statistical difference between the groups at the same concentration (Bonferroni, $p < 0.05$)

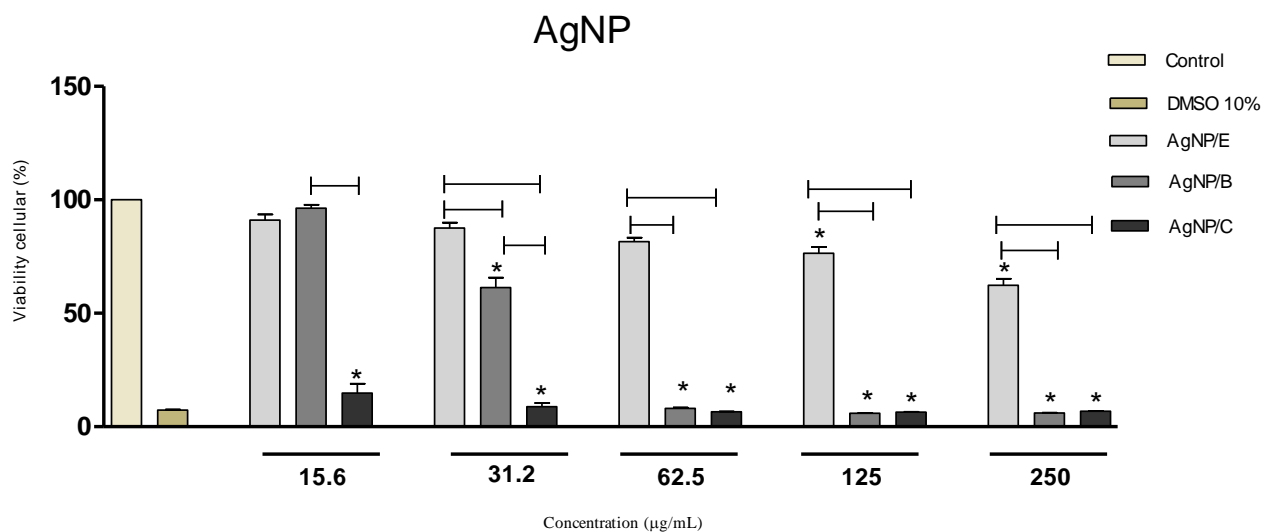


Figure 4. Cell Cytotoxicity obtained by Alamar Blue assay for compounds AgNP/E; AgNP/B; AgNP/C in L929 fibroblast cells. * Indicates statistical differences between the concentration tested and positive control (100% viable cells) and bars indicates statistical difference between the groups at the same concentration (Bonferroni, $p < 0.05$).

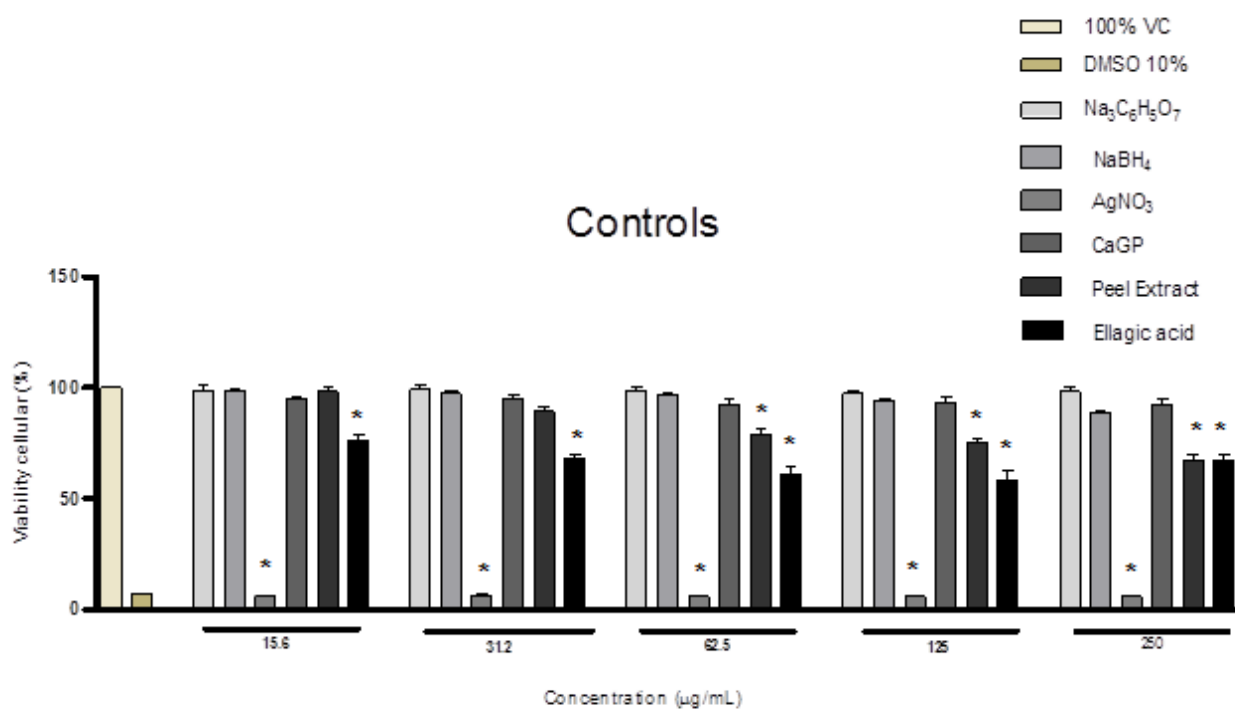


Figure 5. Cell Citotoxicity obtained by Alamar Blue assay for controls in L929 fibroblast cells.* Indicates statistical differences between the concentration tested and positive control (100% viable cells) (Bonferroni, $p < 0.05$)

Anexos

Ensaio de Citotoxicidade - Vermelho Neutro

:

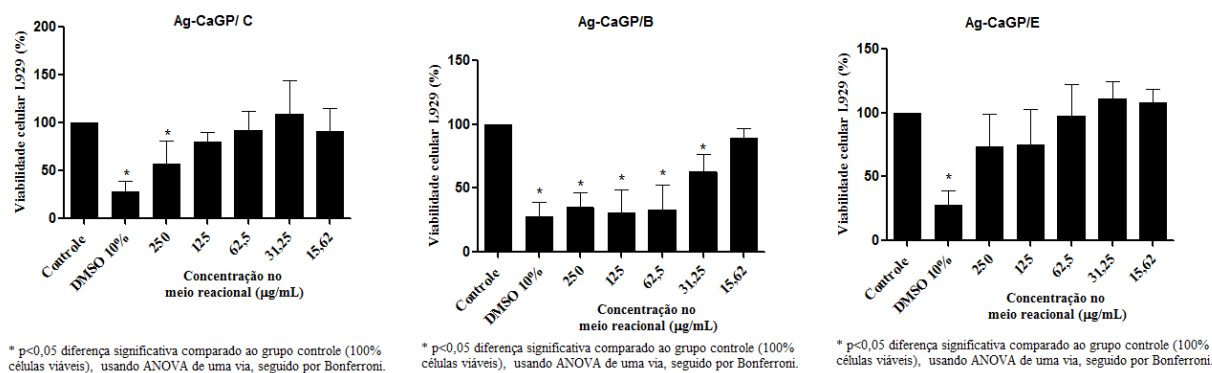


Figura 1. Resultados do ensaio de citotoxicidade celular a partir do teste Vermelho neutro dos nanocompósitos Ag-CaGP/C; Ag-CaGP/B; Ag-CaGP/E.

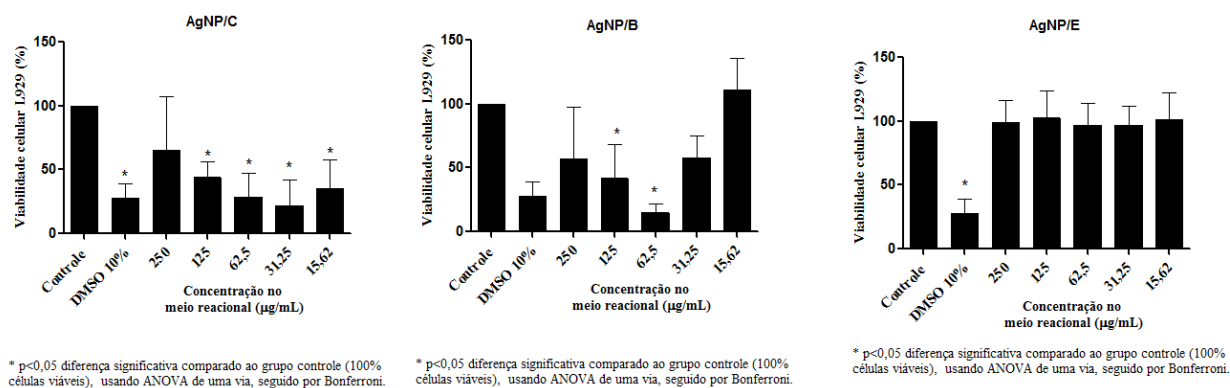
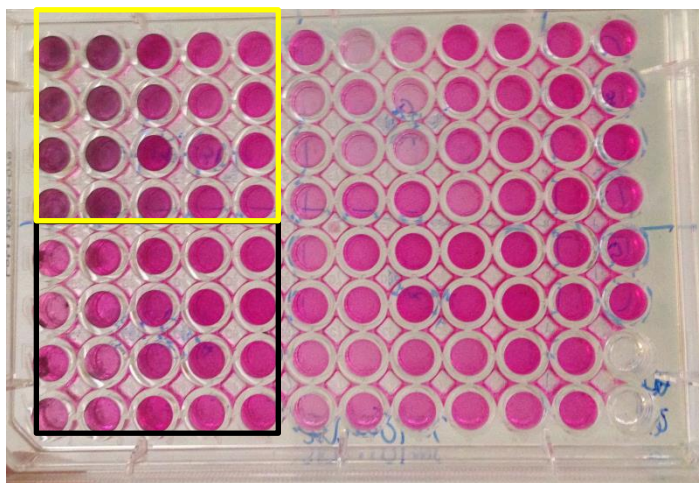


Figura 2. Resultados do ensaio de citotoxicidade celular a partir do teste Vermelho neutro dos nanocompósitos AgNP/C; AgNP/B; AgNP/E.



Fotografia 1. Identificando a coloração dos compostos Ag-CaGP/E em amarelo e AgNP/E em preto, mostrando a possível interferência desse teste nos resultados de citotoxicidade celular.

Ensaio de Cristal Violeta, XTT e CFU em biofilmes em formação simples e misto de *C. albicans* e *S. mutans*

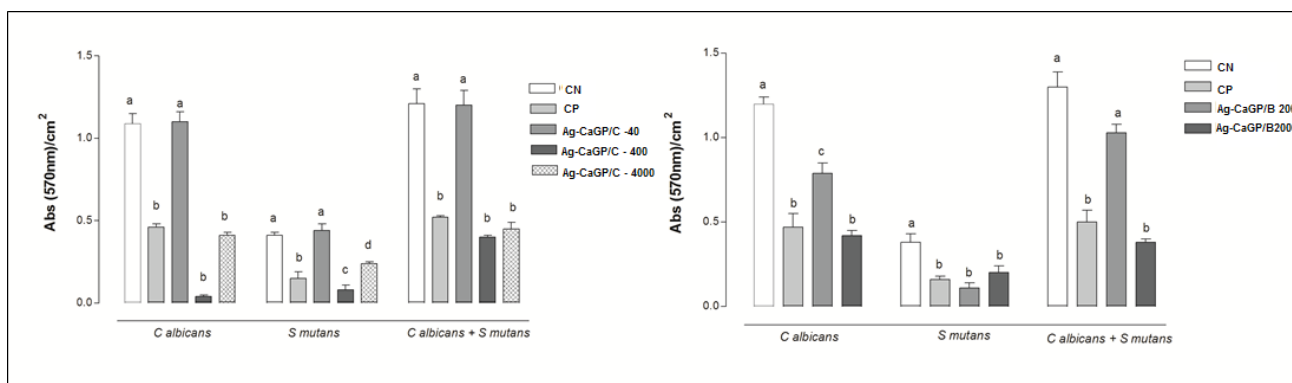


Figura 1 . Valores de absorvância obtidos através do CV para biofilmes simples em formação de *C. albicans* e *S. mutans* . Barras indicam desvio padrão da média. Letras distintas indicam diferença estatística entre os grupos (Fisher, $p < 0.001$).

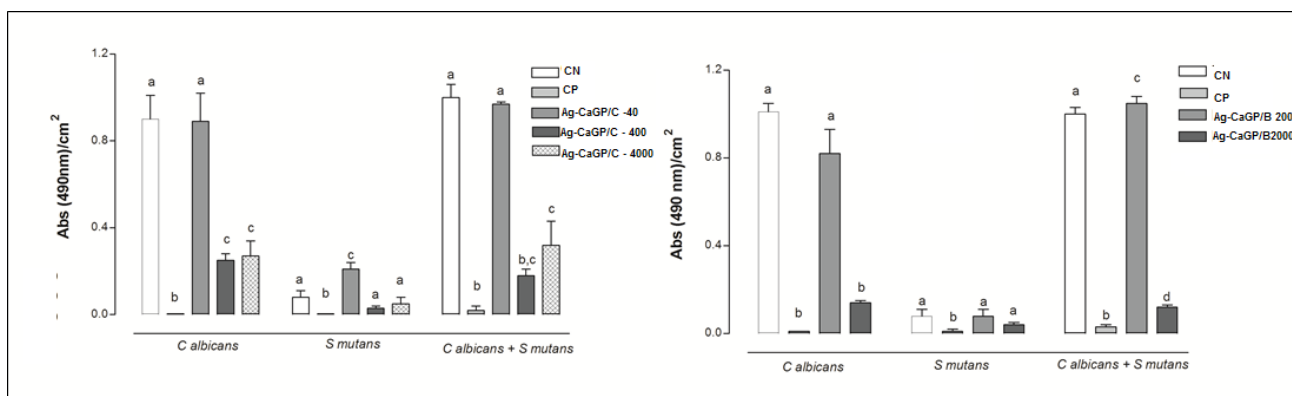


Figura 2 . Valores de absorvância obtidos através do XTT para biofilmes simples em formação de *C. albicans* e *S. mutans* . Barras indicam desvio padrão da média. Letras distintas indicam diferença estatística entre os grupos (Fisher, $p < 0.001$).

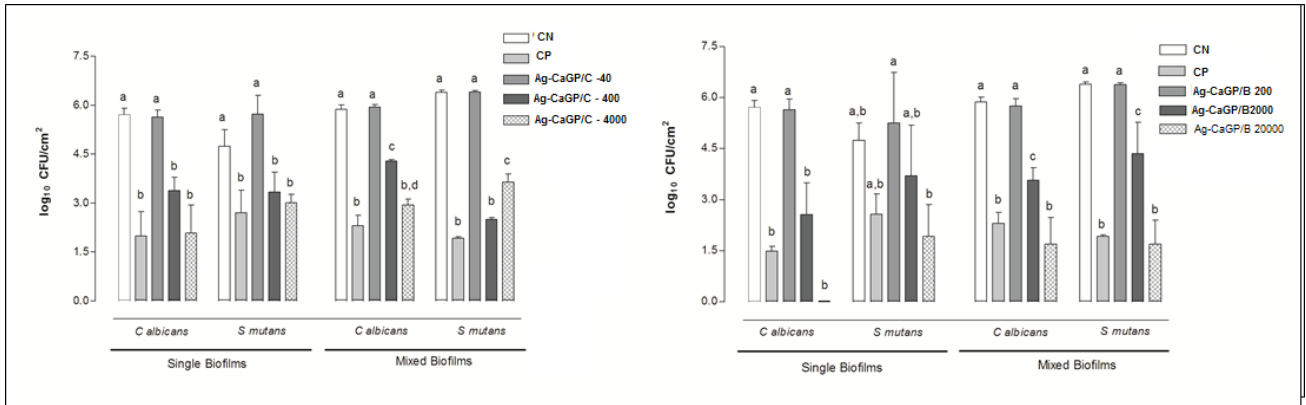


Figura 3 . \log_{10} CFU/cm² obtidos para biofilmes simples em formação de *C. albicans* e *S. mutans* . Barras indicam desvio padrão da média. Letras distintas indicam diferença estatística entre os grupos (Fisher, $p < 0.001$).